

# Composition and Depositional Settings of Lower Cretaceous Terrigenous Rocks of the Kema River Basin, Eastern Sikhote Alin

A. I. Malinovsky, V. V. Golozubov, and V. P. Simanenko

*Far East Geological Institute, Far East Division,  
Russian Academy of Sciences, pr. Stoletiya Vladivostoka 159, Vladivostok, 690022 Russia  
e-mail: malinovsky@fegi.ru*

Received December 10, 2003

**Abstract**—Based on structure, mineralogy, petrography, and geodynamic setting of sedimentation, Barremian(?)–Albian terrigenous rocks in the Kema terrane (Eastern Sikhote Alin) are interpreted as back-arc rocks of the Moneron–Samarga island-arc system. The composition of terrigenous rocks indicates that an ensialic volcanic island arc, the basement of which was composed of the oceanward-advancing continental crust fragment, served as the main source of clastic material. Genetic features of rocks suggest their formation in the lower zone and near the foothill of submarine slope, as well as in adjacent areas of the basin plain. Accumulation of the thick gravitational sequence in the rear zone of the island arc was accompanied by active volcanic processes.

## INTRODUCTION

The study of terrigenous complexes in the Pacific Ocean framing is a reliable tool for understanding geological history of its active continental margins. However, not all aspects of this problem have been elucidated and poor study of these complexes hampers the solution of some issues. This paper analyzes the composition and formation conditions of one of these complexes related to the volcanic island arc.

Lower Cretaceous rocks of Sikhote Alin accumulated in intracontinental basins, marginal seas, and oceans (Markevich *et al.*, 1999, 2000). Of special significance for the paleogeographic reconstruction of Cretaceous evolution of Paleoasia are basins related to volcanic island arcs. In most cases, their island-arc origin was established by petrogeochemical investigations of volcanic rocks (Kovalenko, 1985; Simanenko, 1986, 1991). Data on the composition of sedimentary rocks are scanty and schematic. Therefore, identification of basin type (fore- or back-arc) is a difficult task and reliability of the existing paleotectonic reconstructions is doubtful.

This paper presents data on terrigenous rocks yielded by the comprehensive lithological investigations of Lower Cretaceous rocks of the Kema River basin in the Kema terrane (eastern Sikhote Alin). We studied petrography, proportions of rock-forming components, bulk chemistry, and heavy clastic mineral composition. This information was necessary to determine the provenance composition and paleotectonic setting of sedimentation basins.

## GEOLOGICAL SETTING

The Kema island-arc terrane (Khanchuk *et al.*, 1995) is situated in the eastern Sikhote Alin Ridge and extending as an 80-km-thick band along the coast of the Sea of Japan (Fig. 1). The northwestern Zhuravlev terrane is composed of the Early Cretaceous flysch. Geological relations between these terranes are unknown. Accessible segments of the Kema terrane are exposed as “windows” in basins of the Buta, Mulya, Edinka, Kaban’ya, Samarga, and Kema rivers in the Late Cretaceous (East Sikhote Alin) volcanic belt. The Kema terrane is composed of Barremian–Albian rocks mainly represented by turbidites, mixtite units, mafic volcanic rocks, and their pyroclastic material (Malinovsky *et al.*, 2002). Based on the petrochemical composition of volcanic rocks, Simanenko (1986, 1991) suggested that the Kema terrane is a part of the Early Cretaceous Moneron–Samarga island-arc system. In this paper, we attempted to show the island-arc nature of the terrane based on the study of composition of terrigenous rocks.

## OBJECTS AND METHODS

In the Kema terrane, we investigated Lower Cretaceous rocks of the Meandrovyi and Kema formations located in the Kema River basin. Rocks of the Luzhki Formation were studied in the southern Kema–Taezhnaya interfluve (Fig. 2). We studied ten typical sections (total length more than 20 km) exposed along the Kema River and its tributaries (Kholmogorka, Sitsa, Smekhovka, and Zapadnaya Kema streams). Bedding conditions and structures of rocks were studied in the exposures and polished samples.

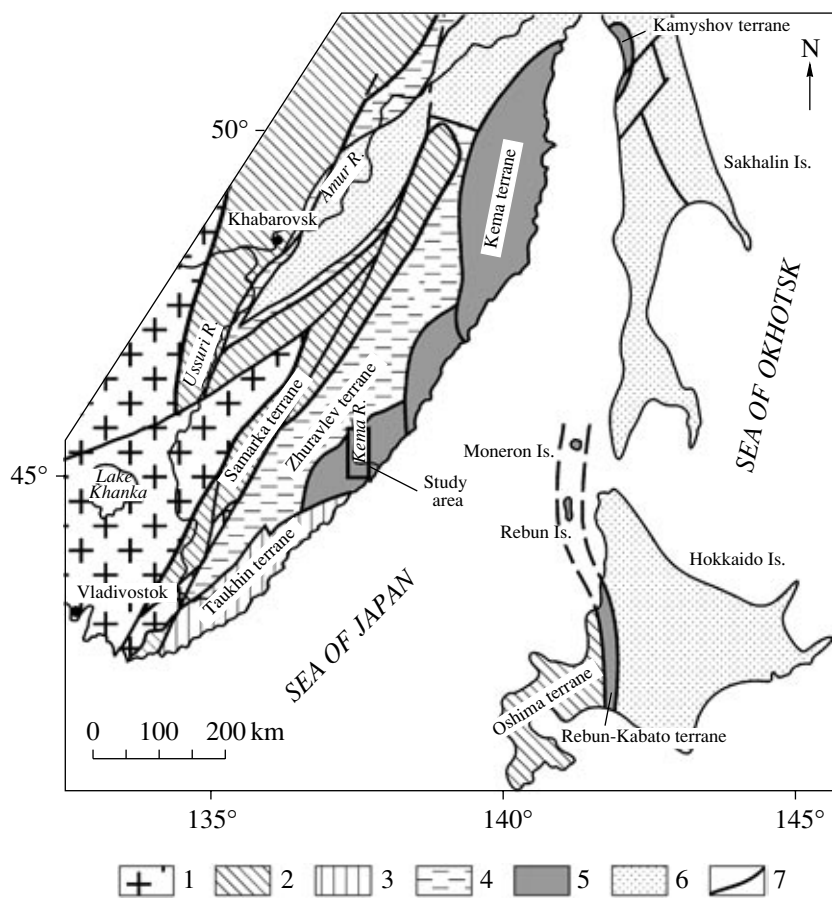


**Fig. 1.** Scheme of terranes in the southern Russian Far East and adjacent territories (Khanchuk *et al.*, 1995; Malinovsky *et al.*, 2002). (1–6) Terranes: (1) Pre-Mesozoic, (2) Jurassic accretionary prisms, (3) Early Cretaceous accretionary prisms, (4) Early Cretaceous turbidite, (5) Early Cretaceous island arc, (6) Cretaceous and Paleogene; (7) faults

Petrography of rocks was studied under polarization microscope. Heavy minerals were separated from sandstones and determined by routine methods. Only clastic minerals were used in calculations, whereas authigenic minerals were excluded for the most reliable determination of the composition and contribution of provenances. The chemical composition of heavy minerals was analyzed on a JXA-5A microprobe. The percentage and chemical composition of heavy minerals were determined using an original technique developed in the Laboratory of Sedimentary Geology of the Far East Geological Institute. This technique makes it possible to recognize paleoanalogues of recent geodynamic settings and to reconstruct different types of island-arc settings (Nechaev *et al.*, 1996; Markevich *et al.*, 1997). The major-element composition of rocks was determined by the traditional chemical method. All analyses were performed in laboratories of the Far East Geological Institute. The age of palynological assemblages was determined by V.S. Markevich at the Biological-Soil Institute of the Far East Division of the Russian Academy of Sciences.

## STRUCTURE AND COMPOSITION OF GEOLOGICAL SECTIONS

The stratigraphy and composition of the Barremian-Albian sequence studied in the Kema River basin is as follows (Fig. 2).

The base of the summary section is represented by the Meandrovi Formation up to 1100 m thick. It consists of a rhythmic alternation of sandstones and siltstones, often grading into silty mudstones and mudstones with elementary rhythm (cyclite) thickness ranging from 3–10 to 20–30 cm (occasionally, up to 50–100 cm). In the lower part of the formation, proportions of sandstones and siltstones in the rhythms are similar or the siltstones slightly predominate (the sandstone/siltstone ratio is 1/1.5–1/3 (occasionally, down to 1/8)). In contrast, the upper part is mainly composed of sandstones (the sandstone/siltstone ratio varies from 2/1 to 10/1). In addition, the rhythms are characterized by graded bedding, sharp lower boundary with erosional marks on the base, and sedimentary structures with elements of the Bouma cycle (*abcde*, *bde*, *bcde*, and *cde*). The alternation is occasionally interrupted by slump deformations or siltstone horizons (up to 90 m thick) with rare intercalations

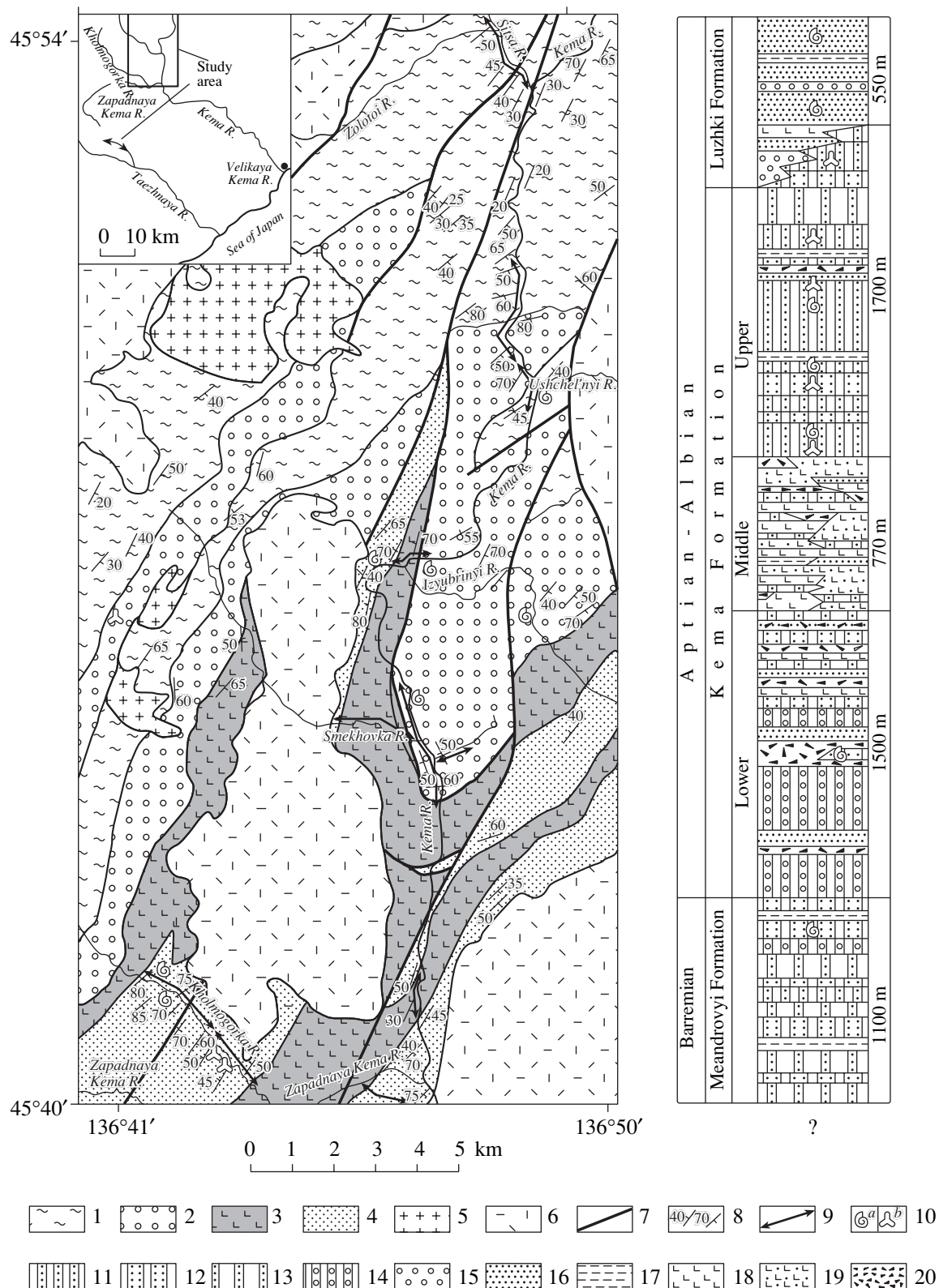


**Fig. 2.** Geological map and lithostratigraphic column of the Kema River basin. Legend for the map: (1) Meandrovyi Formation; (2–4) subformations of the Kema Formation: (2) Lower Kema, (3) Middle Kema, (4) Upper Kema; (5) Late Cretaceous granitoids; (6) volcanic rocks of the Eastern Sikhote Alin belt; (7) faults; (8) dip and strike; (9) studied sections; (10) localities of findings of (a) fauna, (b) spores and pollen. Legend for the column: (11–13) rhythmic alternation of sandstones and siltstones: (11) with equal proportions, (12) with the predominance of sandstone, (13) with the predominance of siltstone; (14) rhythmic alternation of gritstones, sandstones, and siltstones; (15) conglomerates and gritstones; (16) sandstones; (17) siltstones; (18) basalts and basaltic andesites; (19) mafic tuffs and tephroids; (20) mixtites.

tions (5–10 cm) of fine-grained sandstones. The upper section of the Meandrovyi Formation contains gritstones (60 m) laterally grading into coarse-grained sandstones with shapeless fragments of siltstones and plant detritus. Based on few findings of shells of *aucellina* and ammonites, the Meandrovyi Formation is dated as Barremian–early Aptian (Markevich *et al.*, 2000).

The overlying **Kema Formation** is divided into three subformations. The *Lower Kema Subformation* (more than 1500 m thick) is composed of fine-pebble conglomerates, gritstones, inequigranular sandstones, and diverse (in clast size, structure, and composition) mixtites that represent a mixture of clastic unsorted rocks with the content of clastic component less than 80%. Depending on size, shape, and their relations with the sandy–clayey material, they are subdivided into bouldery–pebbly–clayey, sandy–clayey–pebbly, blocky–bouldery–clayey, and other types (Ruzhentsev and Khvorova, 1973; Sokolov, 1977). Less common are packages of rhythmically interstratified sandstones and siltstones in variable proportions, horizons of slump deposits and tuffs, rare basaltic beds (up to 10 m), as well as intercalated up to 80-m-thick beds of 2–6-m thick rhythms consisting of fine-pebble conglomerates, gritstones, and coarse-grained sandstones grading upsection into fine-grained sandstones and siltstones. The *Middle Kema Subformation* (770 m) is mainly composed of basalts, their tuffs, and tephroids. Volcanomictic sandstones, rhythmically intercalated sandstone–siltstone beds, and horizons of slump deposits and mixtites with basaltic blocks (up to 1.5 m) are rare. The *Upper Kema Subformation* (up to 1500 m thick) is mainly composed of rhythmically intercalated beds (30–300 m) of sandstones and siltstones. Rhythms are from 3–10 to 60–100 cm thick. The sandstones and siltstones in rhythms occur in equal proportions, with an occasional predominance of a certain component. Rhythms are dominated by Bouma successions *bde*, *bcde*, *abde*, and *cde*. The monotonous intercalation is occasionally interrupted by thin siltstone horizons with sandstone interbeds and is complicated by slump deformations or mixtites. The *aucellina* and ammonite remains collected from the Kema sequence indicate its early Aptian–late Albian age (Markevich *et al.*, 2000). The same age interval is suggested by the palynological assemblage extracted from the lower and upper subformations (Malinovsky *et al.*, 2002).

The section is completed by the Lower Cretaceous Luzhki Formation (up to 550 m) composed of medium- to fine-grained sandstones with scarce horizons and lenses of conglomerates, gritstones, and siltstones, as well as basaltic andesite and tuff beds in the lower part. Based on numerous findings of molluscs, the Luzhki Formation is dated as middle–late Albian (Markevich *et al.*, 2000) that corresponds to the age of the upper part of the Upper Kema Subformation. Thus, the Luzhki Formation represents a facies analogue of the Upper Kema Subformation.

## COMPOSITION OF TERRIGENOUS ROCKS AND ITS GEODYNAMIC INTERPRETATION

We focused our attention on the chemical composition of sandstones, because they bear the maximal information on the type and composition of provenances and the geodynamic settings of sedimentation areas. We also took into consideration the composition of clayey and coarse-clastic rocks and the chemical composition of heavy minerals from the Kema basalts.

### *Petrographic Composition and Rock-Forming Components of Sandstones*

The studied sandstones are typically fine to medium-grained, occasionally coarse-grained to gravelly rocks. They are well sorted, but the sorting becomes worse with increasing grain size. Sandstones, especially in the Lower Kema Subformation, occasionally contain small (up to 2 cm) shapeless siltstone clasts scattered over the entire volume. Sandy grains are typically angular and subangular, more rarely subrounded. Grains of siliceous and sedimentary rocks are best rounded, while grains of volcanic rocks are least rounded.

In terms of rock-forming components, sandstones have a fairly homogeneous composition corresponding to polymictic rocks. Clasts (60–80 vol %) include quartz, feldspars, terrigenous, siliceous, and volcanic rock fragments, volcanic glass, and ore minerals. In the classification diagram proposed by Shutov (1967), sandstones form a single field mainly ascribed to the feldspar–quartz and quartz–feldspar graywackes, whereas the feldspar-bearing arkoses are subordinate (Fig. 3a).

Quartz is the most abundant component accounting from 30 to 52% (Fig. 3a). The highest (35–52%) and lowest (31–42%) quartz contents were found in the Lower and Middle Kema subformations, respectively. The quartz mainly occurs as monocrystalline volcanic grains. They are pure, elongated angular or subangular grains, often with wavy extinction. Intrusive and metamorphic quartz grains are less common.

The content of feldspars in the sandstones is 22–41%. They are mainly observed as plagioclases (60–95%) dominated by albite and oligoclase. Feldspar grains are typically elongated, tabular, and occasionally equant. K-feldspars (orthoclase and less common microcline) account for up to 20%.

Lithic fragments (17–42 vol %) include siliceous (30–45%) and sedimentary rocks (25–35%) with subordinate mafic volcanics (15–30%). Fragments of intrusive and metamorphic rocks are rare.

Thus, the clastic composition of sandstones indicates that sediments of the Kema River basin were derived from provenances composed of sedimentary and volcanic rocks. The sedimentation was constantly affected by synsedimentary volcanic eruptions that supplied a large amount of pyroclastic material to the Kema Basin.

Paleotectonic interpretation of the composition of rock-forming components was performed using the

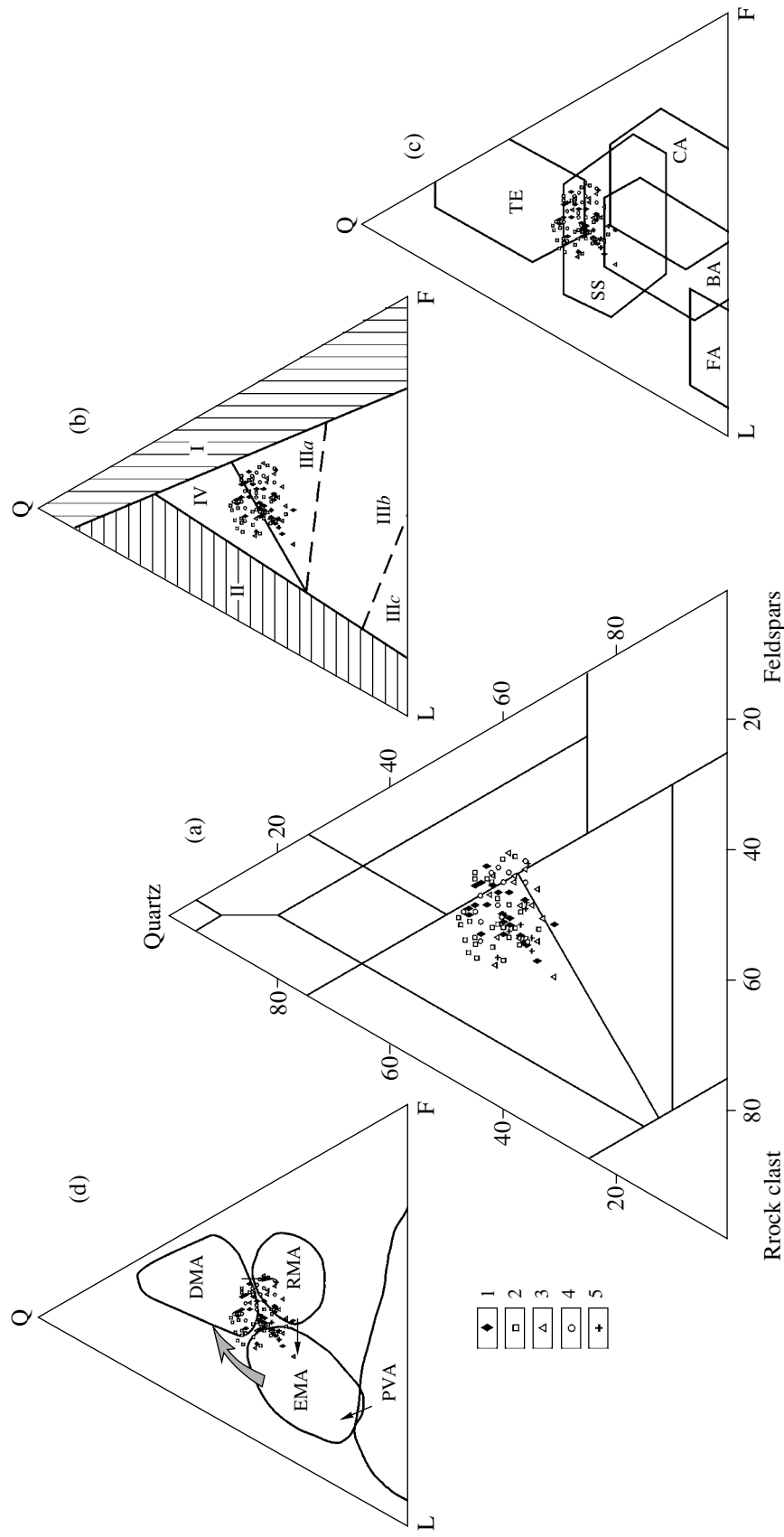


**Fig. 3.** Rock-forming components of sandstones from the Kema River basin and their paleogeodynamic interpretation. (a) Classification diagram of rock types (Shutov, 1967). (b) Source rocks (Dickinson, 1979): (I) magmatic arcs; (II) recycled orogens; (III) continental blocks; (IV) mixed provenances. (c) Basin types (Maynard *et al.*, 1982): (TE) Passive environment (intercontinental rifts and aulacogens); basins of active continental margins conjugated with (SS) strike-slip dislocations; (CA) continental-marginal magmatic arc, and oceanic volcanic arc; (FA) fore-arc, (BA) back-arc. (d) Types of magmatic arcs (Kumon and Kiminami, 1994): (PVA) primitive volcanic arc; (EMA) evolved and mature magmatic arc; (DMA) dissected magmatic arc, (RMA) recycled magmatic arc. Black arrows show evolution and maturation; gray arrows, erosion of upper zones of the arcs and their dissection during erosion. (1–5) Formations: (1) Meandrovyi, (2–4) Kema, Sub-formations: (2) Lower Kema, (3) Middle Kema, (4) Upper Kema, (5) Luzhki.

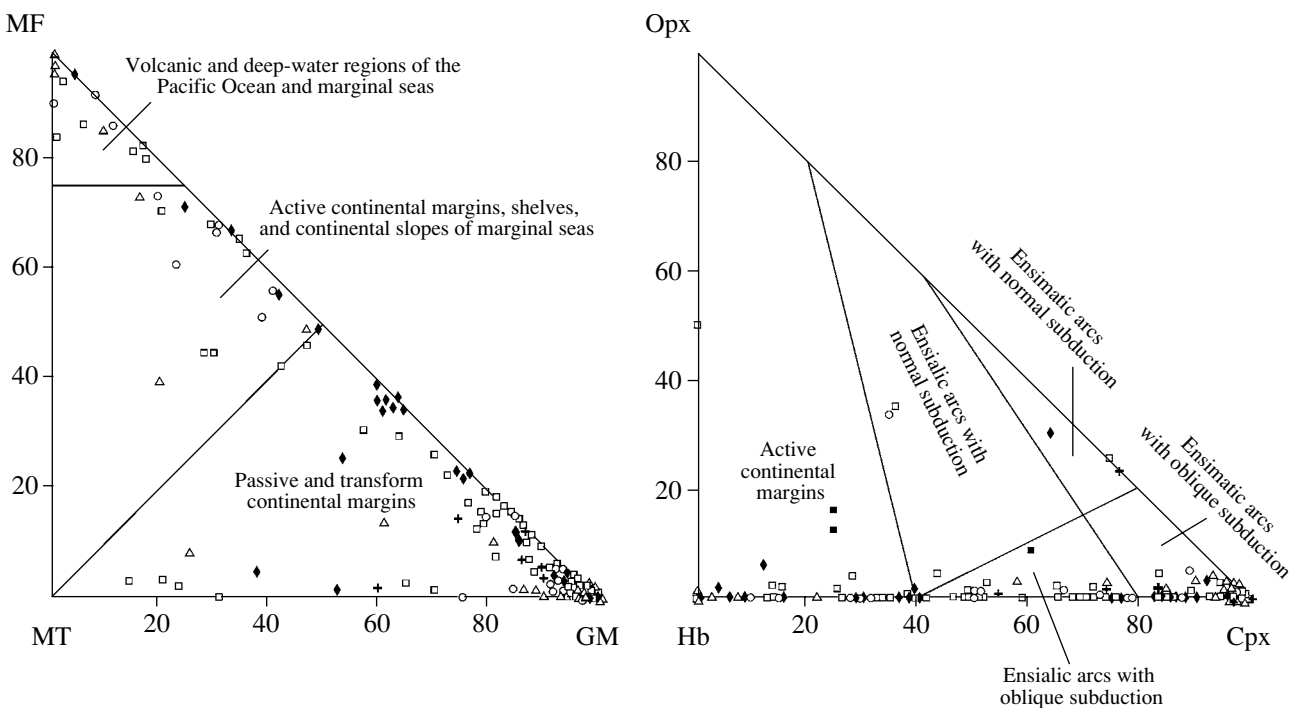


**Fig. 4.** Comparison of heavy fractions from sandstones in the Kema River basin vs. recent sediments in different geodynamic settings (Nechaev *et al.*, 1996). (MF) Total content of olivine, pyroxene, and green hornblende; (MT) total content of epidote, garnet, and blue-green amphiboles; (GM) total content of zircon, tourmaline, staurolite, disthene, sillimanite, and andalusite. (Opx) orthopyroxene, (Hb) hornblende, (Cpx) clinopyroxene. Symbols are as in Fig. 3.

well-known and generally accepted techniques of W. Dickinson, C. Suczek, J. Maynard, F. Kumon, and others. In the diagram of Dickinson and Suczek (1979) that characterizes the tectonic settings of provenances (Fig. 3b), the Kema sandstones are mainly plotted in the field of dissected, deeply eroded, presumably epicontinental island arcs (IIIa) and, to a lesser extent, in the field of mixed provenances including remobilized orogens and mature island arcs (IV). Sandstones, presumably, formed as a result of the disintegration of granitoid intrusions in root zones of arcs and their volcanic envelopment. Geotectonic settings of Early Cretaceous sedimentary basins are reconstructed using the diagram of Maynard *et al.* (1982). In Fig. 3b, data points of the studied sandstones plot in three fields: intercontinental rifts and aulacogens (TE), active continental-margin basins complicated by strike-slip faulting along transform faults (SS), and, partially, back-arc basins of oceanic island arcs (BA). Since the diagram shows a significant overlapping of different fields, additional information is required to determine unambiguously the tectonic type of sedimentary basin. Based on diagrams of Kumon and Kiminami (1994), we attempted to reconstruct the type of magmatic (island) arcs from the clastic composition (Fig. 3d). The Kema sandstones mainly correspond to the well-developed, mature, and strongly eroded arcs.

#### Heavy Minerals of Sandstones

The heavy fraction accounts for 0.01–0.7 vol % (occasionally, up to 3%) in the Kema sandstones. All heavy clastic minerals can be arbitrarily subdivided into two assemblages. The first assemblage (40% of the total content of heavy minerals) includes typical minerals of island-arc volcaniclastic rocks (orthopyroxene, clinopyroxene, hornblende, chromite, and magnetite). The largest content of volcanic assemblage was found in the Middle Kema sandstones (up to 100%). The major mineral is clinopyroxene (up to 98% in some places). The first assemblage also contain hornblendes (up to 55%), orthopyroxenes (up to 3%), chromite (up to 37%), and magnetite (up to 14%). The second assemblage (on average 60% of the heavy fraction) contains felsic minerals, such as zircon, garnet, tourmaline, epidote, apatite, titanite, and rutile. The predominant mineral is zircon (up to 100% in some samples). The second assemblage also contains garnet (up to 77%), tourmaline (up to 18%), and epidote (up to 11%). Other minerals account for a few percents.

It is known that the tectonic settings are characterized by typical heavy mineral assemblages (Markevich *et al.*, 1997; Nechaev *et al.*, 1996; Nechaev and Ispahordig, 1993). Figure 4 shows the distribution of different mineral assemblages from the Kema sandstones in the MF–MT–GM and Opx–Hb–Cpx diagrams (Nechaev *et al.*, 1996). It is evident that the heavy minerals were supplied from two major provenances. The volcanic assemblage corresponds

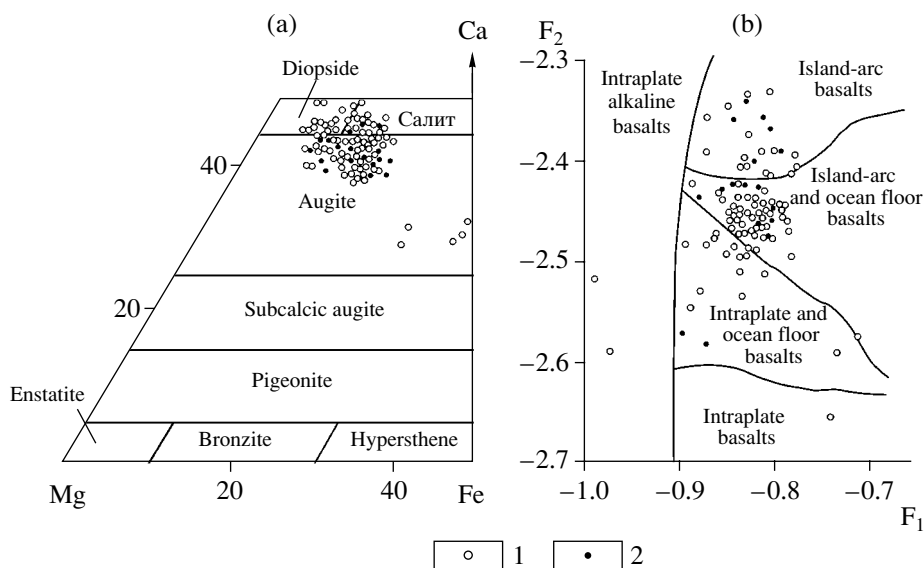


**Fig. 5.** (a) Compositions of clastic clinopyroxenes (in sandstones) and clinopyroxenes (in basalts). (b) Discriminant diagram for clinopyroxenes in basalts from different tectonic settings (Nisbet and Pearce, 1977). (1, 2) Clinopyroxenes in sandstones and basalts, respectively.

$$F_1 = -0.012 \cdot SiO_2 - 0.0807 \cdot TiO_2 + 0.0026 \cdot Al_2O_3 - 0.0012 \cdot FeO - 0.0026 \cdot MnO + 0.0087 \cdot MgO - 0.0128 \cdot CaO - 0.0419 \cdot Na_2O;$$

$$F_2 = -0.0496 \cdot SiO_2 - 0.0818 \cdot TiO_2 - 0.02126 \cdot Al_2O_3 - 0.0041 \cdot FeO - 0.1435 \cdot MnO - 0.0029 \cdot MgO - 0.0085 \cdot CaO + 0.0160 \cdot Na_2O.$$

to an active continental margin and (or) ensialic arc with oblique subduction. The assemblage is mainly related to the erosion of island-arc volcanic rocks. Judging from the upsection decrease in pyroxene and hornblende, the volcanic rocks played a major role in the Middle Kema Subformation, but their contribution decreased with time. The felsic assemblage presumably accumulated near an oceanward-advancing continental crust fragment in the arc basement. An amagmatic transform plate boundary could also take place.

For a more reliable determination of provenances of heavy minerals, we studied the chemical composition of clinopyroxenes, amphiboles, chromites, and garnets (Table 1).

The type of volcanic provenance can most efficiently be determined from the *clinopyroxene* composition. In the diagrams presented, we compared clinopyroxenes from sandstones and basalts of the Meandrovyi and Kema formations. Clinopyroxenes from sandstones form a single field and are very similar to those from basalts. In the Mg–Ca–Fe diagram (Fig. 5a), they correspond to augite, diopside, and salite. In the discriminant diagram (Fig. 5b) based on (Nisbet and Pearce, 1977), most clinopyroxenes from sandstones correspond to those from the volcanic island-arc and, partially, oceanic floor basalts. The Ti–(Ca + Na), (Ti + Cr)–Ca, and Ti–Al diagrams (Leterrier *et al.*, 1982) made it possible to distinguish pyroxenes from basalts of different geodynamic settings with a probability of >80% (Fig. 6). In Fig. 6a, clinopyroxenes (including those from basalts) plot near the discrimination line between alkaline basalts and tholeiites. For-

mally, the clinopyroxenes belong to alkaline basalts. However, they differ from the alkaline basalts in low Ti and Na contents. Figure 6b divides the tholeiitic basalts into MORB basalts, on the one hand, and island-arc and continental-margin (calc-alkaline and tholeiitic) basalts, on the other hand. One can see that clinopyroxenes from sandstones plot in or approximate the island-arc field. Figure 6c divides island-arc clinopyroxenes into calc-alkaline and tholeiitic varieties. It is evident that the studied pyroxenes were supplied from calc-alkaline basalts typical of the rear parts of island arcs. In the diagram for clastic *chromites* from the Kema sandstones (Fig. 7) compiled according to (Arai, 1992), most data points are plotted in the field of island-arc basalts, with a few points falling in the field of highly alkaline intraplate basalts. The essentially island-arc character of provenance is also supported by the fact that *amphiboles* from the heavy fraction are similar to those from the island-arc volcanic rocks (Fig. 8) (Nechaev, 1990). *Garnets* from sandstones mainly correspond to almandine with occasional grossular or spessartite component. They were presumably derived from eroded acid intrusive and volcanic rocks, although the contribution of metamorphic rocks cannot also be ruled out. Garnet was presumably derived from island-arc basement composed of sialic continental crust.

Thus, the heavy mineral composition of sandstones indicates that their clastic material was mainly derived from subalkaline and calc-alkaline basalts of the volcanic island arc, its sialic basement, and oceanic crustal blocks related to the tectonic stacking of rocks.

**Table 1.** Chemical composition (wt %) of accessory minerals in sandstones from the Kema River basin

Sample no.	SiO <sub>2</sub>	TiO <sub>2</sub>	Al <sub>2</sub> O <sub>3</sub>	Cr <sub>2</sub> O <sub>3</sub>	FeO*	MnO	MgO	CaO	Na <sub>2</sub> O	K <sub>2</sub> O	Total
<b>Clinopyroxene</b>											
KM-766/1	51.40	0.56	2.95	—	8.63	0.20	13.80	21.53	0.41	0.02	99.51
KM-766/2	49.53	0.83	5.16	0.28	6.80	0.15	14.02	22.14	0.30	0.02	99.23
KM-770/1	52.77	1.03	1.58	0.03	21.81	0.84	2.60	10.11	8.99	0.01	99.78
KM-770/2	51.81	0.60	4.57	0.65	5.18	0.08	14.90	22.29	0.30	—	100.38
KM-770/3	47.99	2.02	9.19	—	7.70	0.08	13.40	18.57	0.75	—	99.72
KM-770/4	48.71	2.12	9.15	—	7.79	0.10	13.38	18.78	0.73	—	100.75
KM-770/5	52.40	0.48	3.75	0.24	4.05	0.06	16.19	22.11	0.29	—	99.57
KM-832/1	51.81	0.52	3.92	1.12	5.02	0.09	17.10	21.27	0.21	0.01	101.07
KM-832/2	50.26	0.77	4.59	0.04	8.21	0.19	15.08	20.95	0.31	0.01	100.42
KM-832/3	52.52	0.30	2.20	0.35	4.69	0.07	16.75	22.24	0.21	—	99.33
KM-832/4	53.16	0.32	2.14	0.38	4.22	0.04	18.05	21.98	0.17	0.01	100.47
KM-832/5	52.41	0.44	4.08	0.04	14.44	0.50	14.09	12.76	0.58	0.19	99.54
KM-838/1	51.33	0.78	3.36	0.08	8.33	0.25	14.38	20.58	0.42	—	99.51
KM-838/2	50.17	0.94	3.93	0.04	8.48	0.26	14.28	20.59	0.29	—	98.99
KM-839/1	51.37	0.67	2.78	0.26	5.50	0.25	15.84	22.67	0.19	—	99.54
KM-839/2	50.25	0.55	3.88	0.17	6.22	0.18	14.61	23.19	0.21	—	99.25
KM-839/3	50.66	0.63	2.56	0.04	7.96	0.40	15.38	20.69	0.35	—	98.67
KM-839/4	51.87	0.97	1.51	0.01	22.47	0.70	2.69	9.88	9.57	—	99.67
KM-7	50.46	0.52	3.98	0.41	6.13	0.12	16.67	21.80	0.30	—	100.39
KM-10	50.72	0.64	3.04	—	8.32	0.30	15.90	21.52	0.29	—	100.74
KM-15	53.14	0.41	2.89	0.10	6.12	0.17	15.48	22.86	0.23	—	101.41
KM-13/1	53.65	0.72	3.00	0.21	7.71	0.28	15.07	20.76	0.28	—	101.69
KM-13/2	52.05	0.80	5.20	0.53	5.96	0.21	14.54	21.56	0.30	—	101.14
KM-23	51.87	0.68	2.72	—	8.38	0.29	15.71	21.70	0.30	—	101.66
KM-43	48.86	0.75	5.10	0.36	7.29	0.16	14.70	21.86	0.28	0.01	99.38
KM-51/1	49.81	0.82	4.12	0.27	7.35	0.17	15.01	22.08	0.32	0.01	99.96
KM-51/2	50.99	0.51	3.49	0.06	8.56	0.33	14.99	20.73	0.39	—	100.04
KM-52/1	53.20	0.48	2.85	0.86	5.37	0.23	16.64	20.96	0.33	—	100.91
KM-52/2	53.09	0.51	2.91	0.78	4.33	0.17	16.02	22.67	0.24	—	100.72
KM-67/1	51.42	0.60	3.55	0.07	5.51	0.13	15.36	23.73	0.18	—	100.56
KM-67/2	53.04	0.53	2.70	0.28	5.22	0.14	16.21	22.25	0.31	—	100.68
KM-68/1	50.11	0.74	2.60	0.15	8.01	0.24	18.02	20.09	0.34	—	100.31
KM-68/2	50.83	0.72	2.90	0.75	5.12	0.14	18.93	21.32	0.22	—	100.92
KM-68/3	49.63	0.87	3.14	0.14	8.54	0.19	16.92	20.53	0.40	—	100.37
KM-77	50.57	1.04	3.90	—	9.62	0.25	14.23	20.71	0.37	0.01	100.71
KM-78/1	51.65	0.86	2.79	0.04	7.81	0.25	14.17	21.96	0.32	—	99.86
KM-78/2	51.78	0.61	3.60	0.29	7.04	0.13	14.63	22.47	0.30	—	100.86
KM-223/1	49.30	0.90	3.03	0.04	8.59	0.27	15.55	22.10	0.34	—	100.12
KM-223/2	51.11	0.96	2.28	0.02	8.01	0.33	16.79	21.38	0.32	—	101.20
KM-796/1	51.66	0.51	2.13	0.07	9.04	0.26	16.28	18.84	0.19	—	98.98
KM-796/2	52.18	0.38	3.28	0.13	3.96	0.04	16.59	22.49	0.17	—	99.22
KM-815/1	50.27	0.65	2.50	0.09	8.55	0.38	15.58	20.79	0.19	—	99.00
KM-815/2	50.72	0.56	2.57	0.13	9.44	0.43	15.94	19.50	0.26	—	99.54
KM-815/3	51.97	0.36	1.66	0.28	3.92	0.24	16.80	22.80	0.14	0.01	98.16
KM-815/4	50.29	0.75	2.40	—	9.76	0.49	15.33	20.14	0.30	0.01	99.46
KM-819A/1	51.14	0.59	2.44	—	7.10	0.20	15.11	20.96	0.29	0.01	97.85
KM-819A/2	52.06	0.47	2.02	—	8.81	0.39	14.80	20.71	0.29	0.01	99.59
KM-822/1	50.15	0.38	6.77	0.07	14.45	0.49	13.44	13.52	0.57	0.39	100.23
KM-822/2	52.73	0.28	2.56	0.05	18.26	0.50	12.61	13.35	0.52	0.50	101.35
KM-824/1	52.44	0.28	1.72	0.12	4.48	0.12	17.06	22.53	0.09	—	98.83
KM-824/2	52.48	0.31	1.89	0.64	4.45	0.13	16.79	21.80	0.12	—	98.62
KM-824/3	52.66	0.26	1.86	0.53	3.64	0.12	17.09	22.94	0.11	—	99.20

**Table 1.** (Contd.)

Sample no.	SiO <sub>2</sub>	TiO <sub>2</sub>	Al <sub>2</sub> O <sub>3</sub>	Cr <sub>2</sub> O <sub>3</sub>	FeO*	MnO	MgO	CaO	Na <sub>2</sub> O	K <sub>2</sub> O	Total
KM-825/1	51.32	0.59	4.57	—	6.85	0.13	16.29	20.73	0.34	—	100.82
KM-825/2	50.78	0.80	3.93	0.07	7.93	0.24	15.94	19.86	0.28	0.01	99.82
KM-825/3	51.04	0.62	2.32	0.04	9.29	0.31	16.27	19.68	0.17	—	99.74
KM-825/3	51.04	0.62	2.32	0.04	9.29	0.31	16.27	19.68	0.17	—	99.74
KM-82/2	51.88	0.37	3.05	0.28	5.39	0.12	16.43	22.02	0.19	—	99.75
KM-97/1	53.56	0.34	1.42	0.53	4.42	0.14	17.17	22.93	0.24	0.01	100.75
KM-97/2	52.43	0.84	1.85	0.13	8.79	0.25	16.06	20.12	0.34	—	100.80
KM-97/3	52.28	0.75	1.26	0.07	9.02	0.30	15.65	21.28	0.41	0.01	101.03
KM-109/1	52.31	0.71	1.43	0.04	7.98	0.29	15.04	21.35	0.26	0.01	99.42
KM-109/2	51.78	0.78	1.53	0.04	8.30	0.28	15.74	21.11	0.51	0.01	100.06
KM-109/3	50.95	1.09	2.49	0.06	9.52	0.27	14.23	20.73	0.40	—	99.74
KM-109/4	51.11	0.95	2.90	0.07	9.26	0.25	14.77	20.96	0.41	—	100.68
KM-125/1	50.43	0.76	2.55	0.02	8.39	0.26	13.78	22.28	0.29	—	98.77
KM-125/2	49.84	0.87	3.00	—	8.74	0.21	13.32	23.03	0.40	—	99.43
KM-125/3	50.66	0.72	1.88	0.06	8.90	0.25	13.99	21.72	0.31	—	98.49
KM-139/1	50.40	1.42	3.11	0.07	8.28	0.20	13.95	21.30	0.41	—	99.14
KM-139/2	51.07	0.94	2.22	0.04	8.42	0.24	14.04	20.97	0.48	—	98.41
KM-139/3	50.79	0.87	2.67	0.13	8.01	0.21	14.87	21.35	0.28	—	99.16
KM-139/4	51.64	0.92	1.86	0.12	10.98	0.28	14.40	19.61	0.22	—	100.02
KM-142/1	50.38	0.90	3.52	0.03	8.87	0.33	14.01	20.93	0.41	—	99.38
KM-142/2	51.51	0.61	3.39	1.31	2.78	0.12	14.19	25.74	0.16	—	99.79
KM-142/3	50.27	0.56	3.73	0.08	6.09	0.18	15.22	25.02	0.13	—	101.28
KM-142/4	51.09	0.27	2.82	0.57	3.43	0.10	14.87	26.45	0.04	—	99.64
KM-187/1	49.36	0.51	4.50	0.18	6.87	0.17	15.11	23.86	0.14	0.03	100.74
KM-187/2	49.11	0.66	5.07	0.20	5.76	0.15	12.37	25.43	0.15	—	98.90
<b>Amphibole</b>											
KM-770	46.61	1.86	6.24	0.09	19.61	0.26	10.34	9.71	3.27	0.35	98.33
KM-779/1	43.20	1.03	12.58	0.03	13.97	0.13	12.21	10.40	1.95	0.35	95.85
KM-779/2	42.93	1.16	13.16	—	14.18	0.13	12.18	10.06	1.93	0.38	96.12
KM-832	41.92	1.64	12.32	0.02	12.90	0.26	14.37	11.82	2.03	1.18	98.45
KM-838	43.81	1.32	12.42	0.02	13.46	0.53	12.75	9.88	1.84	0.82	96.85
KM-839	47.97	0.66	5.05	0.05	19.56	0.30	11.73	9.96	2.15	0.11	97.64
KM-7	44.49	0.59	10.20	0.10	14.83	0.27	13.14	12.30	1.50	1.06	98.47
KM-10	46.12	0.84	12.15	0.14	13.05	0.22	13.37	12.19	1.14	0.50	99.71
KM-11/1	44.54	1.32	10.64	0.05	15.04	0.40	11.09	11.71	1.75	1.23	98.58
KM-11/2	43.43	0.56	15.22	0.09	14.20	0.23	11.96	11.39	1.57	0.36	99.00
KM-11/3	44.28	0.82	14.70	0.07	14.10	0.17	11.11	8.88	1.49	0.23	95.84
KM-11/4	42.91	0.80	14.92	0.14	13.99	0.24	11.21	10.93	1.68	0.31	97.13
KM-15	43.77	1.36	13.32	0.05	16.25	0.33	8.91	11.15	1.36	0.94	97.45
KM-18	42.14	1.15	12.70	—	19.94	0.56	9.26	11.95	1.60	1.82	101.11
KM-23	44.11	0.70	15.54	0.10	14.20	0.18	12.18	11.05	1.68	0.32	100.04
KM-52/1	42.35	1.25	11.88	—	19.11	0.48	8.65	11.77	1.55	1.78	98.82
KM-52/2	46.46	0.60	9.98	0.03	13.10	0.31	12.46	12.18	1.46	0.82	97.41
KM-59/1	45.22	0.79	14.48	0.01	13.51	0.19	10.88	10.87	1.66	0.32	97.94
KM-59/2	47.50	0.86	12.15	0.05	12.60	0.24	11.59	11.79	1.36	0.54	98.68
KM-59/3	44.33	0.96	9.92	0.22	15.66	0.29	12.23	11.24	1.87	1.12	97.84
KM-59/4	43.97	0.85	10.00	0.24	15.55	0.36	11.81	11.56	1.74	1.33	97.39
KM-67/1	46.18	0.63	4.67	0.32	13.50	0.31	16.71	11.23	1.08	0.82	95.45
KM-67/2	42.27	0.96	7.85	0.43	14.28	0.30	16.02	10.71	1.65	1.30	95.78
KM-72/1	46.32	0.93	7.82	0.23	14.68	0.33	12.53	11.71	1.39	1.05	96.99
KM-72/2	42.40	0.68	10.92	0.06	18.53	0.30	9.83	11.26	1.36	1.33	96.65
KM-77/1	44.67	0.83	15.03	0.01	13.75	0.31	10.84	10.50	1.48	0.27	97.68
KM-77/2	47.96	0.39	7.54	0.15	12.38	0.28	15.13	12.01	0.94	0.69	97.46

**Table 1.** (Contd.)

Sample no.	SiO <sub>2</sub>	TiO <sub>2</sub>	Al <sub>2</sub> O <sub>3</sub>	Cr <sub>2</sub> O <sub>3</sub>	FeO*	MnO	MgO	CaO	Na <sub>2</sub> O	K <sub>2</sub> O	Total
KM-78	44.29	0.97	9.82	0.25	15.50	0.30	11.76	11.39	1.46	1.14	96.87
KM-201/1	48.54	0.77	5.83	0.03	14.94	—	12.93	10.95	0.43	0.22	94.63
KM-201/2	44.88	1.27	8.58	0.04	15.15	—	12.99	10.32	1.32	0.51	95.06
KM-223/1	45.42	1.04	10.88	0.05	19.40	—	7.88	11.05	1.55	0.88	98.12
KM-223/2	47.70	0.62	8.65	0.07	13.15	—	13.54	11.57	1.44	0.81	97.55
KM-819A	51.46	0.51	2.95	0.02	15.36	0.51	14.76	13.67	0.34	0.09	99.65
KM-824/1	41.74	3.15	10.34	0.06	12.74	0.32	13.49	11.10	2.31	0.93	96.19
KM-824/2	41.87	3.15	10.74	0.05	12.70	0.28	13.26	10.61	2.40	0.94	96.01
KM-825/1	45.61	1.11	10.97	0.09	14.85	0.23	12.03	11.08	2.11	0.29	98.37
KM-825/2	43.91	1.00	13.14	0.06	14.87	0.23	12.96	10.36	1.90	0.37	98.81
KM-82	41.76	0.93	14.01	0.05	15.84	0.34	10.01	11.04	1.24	0.74	95.95
KM-108/1	45.15	0.84	14.33	0.05	13.61	0.24	11.30	10.65	1.60	0.36	98.14
KM-108/2	45.77	0.93	9.28	0.20	15.49	0.34	12.02	11.90	1.56	1.19	98.68
KM-108/3	45.33	0.84	13.46	0.03	13.57	0.21	11.27	10.74	1.50	0.34	97.28
KM-109/1	40.11	2.56	7.26	0.02	18.02	0.41	10.69	11.33	3.62	1.56	95.59
KM-109/2	43.43	1.47	9.80	0.34	20.04	0.35	8.38	11.75	1.90	1.08	98.55
KM-125/1	46.59	0.45	8.35	0.08	12.81	0.25	13.11	13.09	1.32	0.72	96.77
KM-125/2	46.87	0.47	7.92	0.03	12.70	0.27	12.97	12.77	1.34	0.78	96.12
KM-571	43.15	1.48	10.18	—	17.37	0.26	9.37	11.85	2.14	0.52	96.31
KM-142/1	43.05	1.21	10.70	0.26	14.80	0.35	10.41	12.98	1.99	1.44	97.20
KM-142/2	43.13	1.04	11.28	0.28	14.61	0.34	10.23	12.94	1.75	1.21	96.81
<b>Chromite</b>											
KM-759/1	n.a.	0.43	14.44	48.35	28.09	0.38	8.70	n.a.	n.a.	n.a.	100.40
KM-759/2	n.a.	0.36	9.71	53.78	28.83	0.45	7.59	n.a.	n.a.	n.a.	100.72
KM-759/3	n.a.	0.47	12.20	51.13	28.70	0.40	8.50	n.a.	n.a.	n.a.	101.41
KM-776/1	n.a.	0.62	14.60	48.74	22.92	0.24	13.57	n.a.	n.a.	n.a.	100.70
KM-776/2	n.a.	1.73	21.89	38.28	28.47	0.22	11.22	n.a.	n.a.	n.a.	101.82
KM-835/1	n.a.	0.63	12.42	52.40	24.63	0.24	10.57	n.a.	n.a.	n.a.	100.90
KM-835/2	n.a.	1.45	30.65	29.80	26.99	0.11	12.78	n.a.	n.a.	n.a.	101.79
KM-835/3	n.a.	1.61	20.34	38.49	31.61	0.30	5.92	n.a.	n.a.	n.a.	98.28
KM-835/4	n.a.	1.45	24.05	38.57	22.38	0.15	13.18	n.a.	n.a.	n.a.	99.80
KM-839/1	n.a.	0.52	6.62	61.22	21.35	0.29	9.91	n.a.	n.a.	n.a.	99.92
KM-839/2	n.a.	0.93	14.77	42.82	30.53	0.22	10.81	n.a.	n.a.	n.a.	100.08
KM-10	n.a.	0.49	19.72	46.65	24.96	0.03	8.50	n.a.	n.a.	n.a.	100.36
KM-34/1	n.a.	0.51	3.24	62.94	22.55	0.03	8.99	n.a.	n.a.	n.a.	98.26
KM-34/2	n.a.	0.70	13.80	42.77	28.50	0.02	13.33	n.a.	n.a.	n.a.	99.12
KM-41/1	n.a.	0.33	11.98	47.22	26.50	0.02	13.22	n.a.	n.a.	n.a.	99.29
KM-41/2	n.a.	0.40	15.13	53.52	20.31	0.02	10.87	n.a.	n.a.	n.a.	100.26
KM-51/1	n.a.	0.57	14.30	47.80	21.44	0.22	14.44	n.a.	n.a.	n.a.	98.78
KM-51/2	n.a.	0.30	11.39	55.70	14.40	0.19	16.09	n.a.	n.a.	n.a.	98.08
KM-67/1	n.a.	0.28	22.99	30.91	32.41	0.02	12.66	n.a.	n.a.	n.a.	99.27
KM-67/2	n.a.	0.28	19.48	36.21	32.55	0.02	12.85	n.a.	n.a.	n.a.	101.40
KM-68/1	n.a.	0.30	7.54	55.71	20.94	0.32	14.48	n.a.	n.a.	n.a.	99.30
KM-68/2	n.a.	0.26	9.47	55.50	19.59	0.32	13.84	n.a.	n.a.	n.a.	98.99
KM-78/1	n.a.	0.56	16.54	48.03	19.95	0.22	14.09	n.a.	n.a.	n.a.	98.60
KM-78/2	n.a.	0.57	13.53	49.19	27.95	0.32	8.82	n.a.	n.a.	n.a.	100.39
KM-797/1	n.a.	0.87	13.13	48.97	30.71	0.37	6.19	n.a.	n.a.	n.a.	100.24
KM-797/2	n.a.	0.38	4.18	64.52	21.62	0.31	9.32	n.a.	n.a.	n.a.	100.33
KM-797/3	n.a.	0.36	23.79	44.30	18.02	0.24	13.21	n.a.	n.a.	n.a.	99.93
KM-797/4	n.a.	0.70	7.76	56.71	29.29	0.48	6.79	n.a.	n.a.	n.a.	101.74
KM-801/1	n.a.	0.82	7.65	54.33	29.03	0.37	8.30	n.a.	n.a.	n.a.	100.51
KM-801/2	n.a.	0.93	10.70	49.85	29.21	0.29	9.86	n.a.	n.a.	n.a.	100.87
KM-801/3	n.a.	0.93	14.60	44.89	30.73	0.30	8.48	n.a.	n.a.	n.a.	99.93

**Table 1.** (Contd.)

Sample no.	SiO <sub>2</sub>	TiO <sub>2</sub>	Al <sub>2</sub> O <sub>3</sub>	Cr <sub>2</sub> O <sub>3</sub>	FeO*	MnO	MgO	CaO	Na <sub>2</sub> O	K <sub>2</sub> O	Total
KM-816/1	n.a.	0.90	25.82	40.52	17.56	0.15	15.13	n.a.	n.a.	n.a.	100.09
KM-816/2	n.a.	0.68	36.91	29.00	16.90	0.11	16.98	n.a.	n.a.	n.a.	100.59
KM-816/3	n.a.	1.73	7.91	50.08	34.40	0.42	6.36	n.a.	n.a.	n.a.	100.91
KM-819A	n.a.	0.58	8.82	54.73	22.67	0.27	12.16	n.a.	n.a.	n.a.	99.23
KM-824/1	n.a.	0.89	14.96	44.54	29.27	0.29	11.22	n.a.	n.a.	n.a.	101.18
KM-824/2	n.a.	0.66	9.72	54.71	22.63	0.30	12.65	n.a.	n.a.	n.a.	100.68
KM-825/1	n.a.	0.19	21.22	50.54	16.04	0.23	12.89	n.a.	n.a.	n.a.	101.11
KM-825/2	n.a.	1.74	18.76	42.49	30.94	0.35	7.20	n.a.	n.a.	n.a.	101.49
KM-109/1	n.a.	0.76	11.03	52.89	21.13	0.28	13.53	n.a.	n.a.	n.a.	99.64
KM-109/2	n.a.	1.08	7.71	53.41	30.75	0.36	6.95	n.a.	n.a.	n.a.	100.31
KM-571	n.a.	0.75	8.42	52.63	26.28	0.19	11.54	n.a.	n.a.	n.a.	99.83
KM-142	n.a.	0.71	11.36	47.36	32.87	0.41	8.43	n.a.	n.a.	n.a.	101.13
KM-143/1	n.a.	0.44	7.92	57.79	21.86	0.33	12.52	n.a.	n.a.	n.a.	100.87
<b>Garnet</b>											
KM-759/1	37.96	0.23	20.45	0.04	31.35	1.20	5.86	2.05	0.01	0.01	99.16
KM-759/2	37.60	0.19	21.11	0.07	34.63	3.61	2.44	1.17	0.06	0.01	100.90
KM-759/3	38.51	0.18	20.34	0.12	33.14	1.24	4.49	1.25	0.02	0.01	99.30
KM-776/1	38.55	0.07	18.96	—	29.05	8.99	0.56	3.15	0.01	0.01	99.37
KM-776/2	39.09	0.13	19.86	—	33.94	0.52	3.62	2.06	—	0.01	99.23
KM-776/3	38.33	0.11	20.18	0.04	33.47	0.69	5.38	0.87	0.07	—	99.15
KM-838/1	38.58	0.15	22.00	0.08	29.71	0.62	7.99	1.15	0.01	0.01	100.30
KM-838/2	38.10	0.15	21.40	0.14	31.76	1.33	5.48	1.20	—	—	99.56
KM-839/1	37.50	0.10	20.30	0.02	32.95	0.50	3.80	2.93	0.02	—	98.13
KM-839/2	36.59	0.08	20.93	0.04	33.41	2.15	3.14	2.16	0.04	0.01	98.55
KM-839/3	36.03	0.16	19.80	0.04	27.52	12.88	2.55	0.69	0.03	0.01	99.70
KM-35	38.05	0.28	21.87	0.06	35.65	0.35	4.12	0.57	0.02	—	100.98
KM-43	37.76	0.36	20.34	0.09	29.81	1.45	1.63	8.80	0.01	—	100.26
KM-78	41.48	0.17	20.27	0.09	27.33	0.63	9.60	0.92	0.01	—	100.51
KM-813/1	36.65	0.10	20.92	0.05	29.02	4.53	1.60	3.63	0.03	—	96.54
KM-813/2	37.27	0.21	20.09	—	25.31	15.73	0.52	0.17	0.09	0.01	99.41
KM-813/3	37.11	0.11	20.00	—	28.20	10.22	0.91	0.62	0.06	—	97.23
KM-815/1	38.47	0.23	19.65	0.03	34.67	0.80	2.85	3.38	0.01	—	100.01
KM-815/2	39.16	0.35	19.81	0.03	29.62	0.78	8.21	2.75	—	0.01	100.72
KM-815/3	38.38	0.22	19.70	0.11	34.32	0.70	4.74	1.08	0.04	0.01	99.30
KM-815/4	38.10	0.45	19.41	0.10	34.23	1.34	5.28	1.51	—	0.02	100.42
KM-819A/1	37.29	0.17	20.60	0.01	24.09	17.84	—	0.42	0.04	0.02	100.47
KM-819A/2	37.96	0.08	20.86	0.01	34.46	1.34	3.25	1.25	0.05	0.01	99.26
KM-819A/3	38.73	0.07	21.28	0.02	31.59	0.98	5.71	0.98	0.02	0.02	99.40
KM-819A/4	36.88	0.11	19.51	—	29.72	11.89	0.18	0.34	0.06	0.01	98.71
KM-825/1	38.82	0.31	18.21	0.11	21.52	14.18	1.30	6.77	0.06	0.01	101.29
KM-825/2	39.20	0.18	17.57	0.04	32.74	0.86	0.96	7.52	0.04	0.01	99.14
KM-825/3	38.77	0.54	14.08	0.06	17.30	22.22	0.69	5.64	0.05	0.02	99.37
KM-94/1	38.39	0.20	21.69	0.07	30.96	0.56	7.30	1.22	0.07	0.02	100.46
KM-94/2	38.53	0.25	21.12	0.09	32.88	1.52	5.04	1.18	0.06	—	100.67
KM-94/3	39.29	0.23	21.21	0.01	24.04	1.20	8.49	6.13	0.06	0.01	100.68
KM-109/1	40.08	0.22	20.98	0.05	31.80	0.94	5.06	1.60	—	—	100.73
KM-109/2	41.42	0.15	20.99	0.08	26.93	2.10	5.68	4.42	—	—	101.78
KM-109/3	37.70	0.06	0.89	0.03	28.24	0.28	—	31.99	—	—	99.20
KM-571/1	37.90	0.33	19.44	0.08	36.02	1.15	3.39	0.84	—	0.01	99.15
KM-571/2	36.29	0.15	19.74	0.04	25.37	16.42	0.17	1.16	—	—	99.35
KM-173/1	38.91	0.33	21.45	0.14	33.16	0.98	5.21	1.32	—	0.01	101.50
KM-173/2	38.94	0.29	20.72	0.04	31.03	0.90	7.09	1.59	0.07	0.02	100.68

Note: (FeO\*) total iron; (—) not detected; (n.a.) not analyzed. Analyses were performed on a JXA microprobe at the Far East Geological Institute (V. I. Sapin and N. I. Ekimova, analysts).

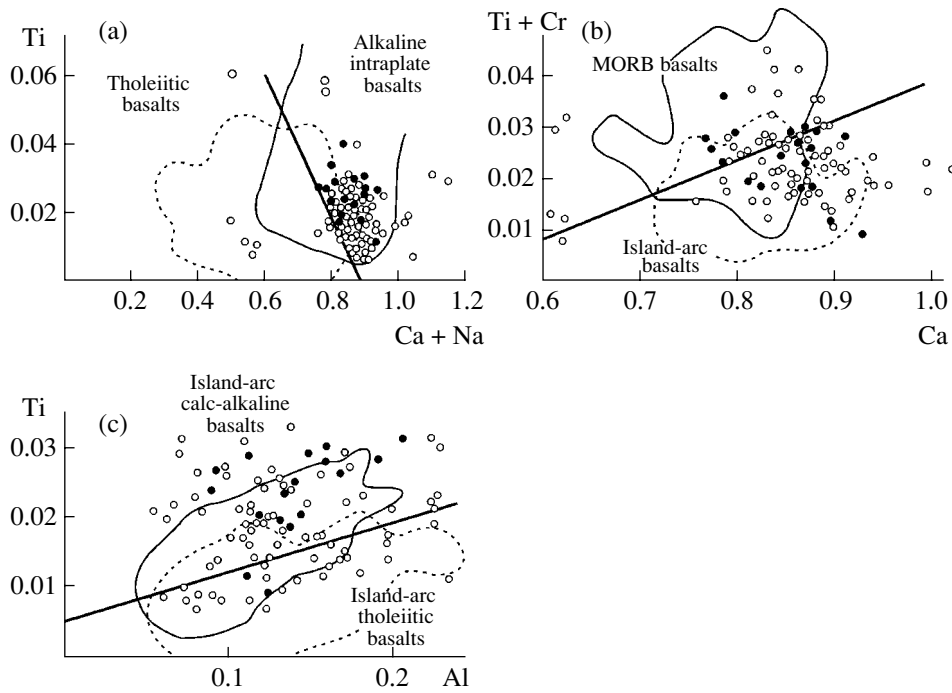


**Fig. 6.** Discriminant diagrams for clinopyroxenes in basalts from different geodynamic settings (Leterrier *et al.*, 1982). Compositional fields of clinopyroxenes from different basalts are shown by solid and dashed lines, respectively. Elements are given in formula units. Symbols are as in Fig. 5.

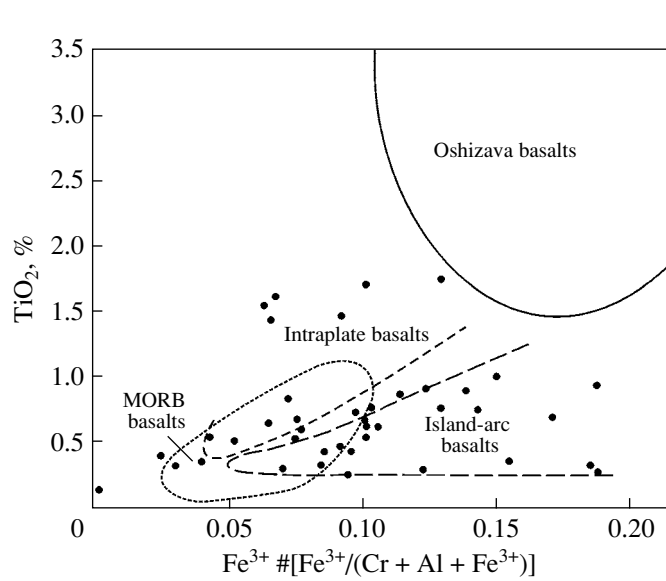


**Fig. 7.** Discriminant diagram for clastic chromites in sandstones from the Kema River and basalts from different tectonic settings (Arai, 1992).

#### Chemical Composition of Sandstones

Sandstones from the Kema River basin have a homogeneous chemical composition (%):  $\text{SiO}_2$  65–83,  $\text{TiO}_2$  0.12–0.66,  $\text{Al}_2\text{O}_3$  6.30–13.92,  $(\text{FeO} + \text{Fe}_2\text{O}_3)$  0.98–5.52,  $\text{MgO}$  0.20–3.12,  $\text{CaO}$  0.14–5.19,  $\text{Na}_2\text{O}$  0.15–3.52, and  $\text{K}_2\text{O}$  0.94–4.04. Such distribution of

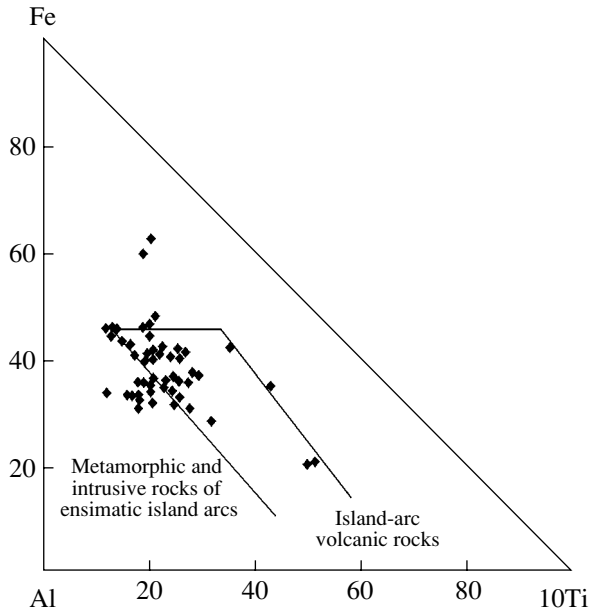


**Fig. 8.** Diagrams of composition of clastic amphiboles from sandstones of the Kema River and their possible volcanic sources (Nechaev, 1991).

major oxides indicates the composition of sandstones is intermediate between arkoses and graywakes. The chemical composition, proportions of rock-forming components, and heavy mineral composition of sandstones depend on source rock composition, which, in

**Table 2.** Chemical composition (wt %) of terrigenous rocks from the Kema River basin

Sample no.	SiO <sub>2</sub>	TiO <sub>2</sub>	Al <sub>2</sub> O <sub>3</sub>	Fe <sub>2</sub> O <sub>3</sub>	FeO	MnO	MgO	CaO	Na <sub>2</sub> O	K <sub>2</sub> O	P <sub>2</sub> O <sub>5</sub>	L.O.I.	H <sub>2</sub> O <sup>-</sup>	Total
<b>Sandstones</b>														
Meandrovyi Formation														
KM-908	75.50	0.23	9.19	0.82	1.64	0.14	1.19	2.84	2.37	1.76	0.04	3.68	0.17	99.57
KM-921	73.87	0.24	10.31	1.12	2.16	0.14	0.02	4.23	1.84	1.64	0.12	3.96	0.15	99.80
KM-927	77.05	0.12	8.98	1.30	1.14	0.05	0.55	2.77	1.97	1.36	0.06	3.97	0.18	99.50
KM-930	76.68	0.26	8.52	1.32	1.29	0.04	0.68	2.08	2.04	1.57	0.21	4.52	0.40	99.61
KM-931	64.16	0.44	12.06	2.38	3.14	0.06	3.01	3.70	2.80	1.28	0.13	5.79	0.46	99.68
KM-934	70.51	0.35	10.36	1.37	2.79	0.07	1.68	3.09	2.61	1.51	0.15	5.07	0.25	99.81
KM-940	74.69	0.27	9.10	0.96	2.88	0.05	0.95	1.83	2.13	1.23	0.16	5.14	0.25	99.64
KM-946	72.14	0.37	10.17	3.37	1.09	0.07	1.22	2.19	2.57	1.47	0.19	4.56	0.36	99.77
KM-950	71.71	0.35	10.50	1.57	1.37	0.08	0.83	3.16	2.58	1.57	0.19	5.37	0.35	99.63
KM-953	72.85	0.40	10.44	0.89	2.36	0.07	0.96	1.95	2.40	1.74	0.19	5.44	0.23	99.92
KM-760	72.30	0.46	7.86	2.92	1.23	0.08	1.72	3.83	2.00	1.39	0.12	5.92	0.38	100.01
KM-762	69.08	0.23	10.26	6.41	1.28	0.08	2.07	1.97	2.62	0.99	0.09	4.49	0.24	99.81
KM-768	72.81	0.27	9.55	2.08	2.01	0.08	1.50	2.51	2.25	1.56	0.11	4.77	0.23	99.73
KM-772	75.47	0.40	10.61	1.68	2.04	0.04	1.06	0.78	2.45	1.97	0.17	2.80	0.27	99.74
KM-782	71.73	0.35	11.70	1.09	3.37	0.05	1.30	1.90	2.34	2.04	0.16	4.14	0.27	100.39
KM-787	82.97	0.17	8.13	1.47	0.51	0.05	0.53	0.39	2.67	1.41	0.08	1.60	0.30	100.28
KM-789	81.95	0.21	8.31	1.04	0.89	0.05	0.63	0.51	2.51	1.51	0.06	1.68	0.28	99.63
KM-791	78.45	0.25	9.95	1.68	0.89	0.04	0.89	0.52	2.56	1.98	0.13	2.76	0.25	100.35
KM-792	78.38	0.35	10.47	2.48	0.80	0.03	1.09	0.63	2.35	1.90	0.13	0.39	0.51	99.51
KM-833	76.19	0.34	11.12	2.89	0.80	0.02	1.06	0.59	2.25	2.06	0.17	1.70	0.36	99.56
KM-835	72.60	0.26	8.65	1.31	3.64	0.16	2.00	2.94	1.78	1.57	0.16	4.02	0.38	99.47
Kema Formation														
Lower Subformation														
KM-4	79.20	0.16	6.21	1.45	1.80	0.11	1.29	3.59	1.06	0.94	0.08	3.37	0.18	99.44
KM-6/A	76.09	0.37	10.90	2.61	0.82	0.03	2.01	0.14	1.50	1.71	0.11	2.72	0.78	99.79
KM-7	81.71	0.14	7.42	1.63	0.71	0.03	0.79	1.65	1.20	1.13	0.06	2.72	0.18	99.37
KM-10	71.84	0.43	12.28	0.85	3.82	0.04	1.50	1.25	2.30	1.35	0.15	3.27	0.43	99.51
KM-17	78.66	0.26	8.77	1.41	1.72	0.05	1.20	2.10	1.10	1.24	0.10	3.07	0.23	99.91
KM-18	79.84	0.29	6.77	2.05	1.23	0.12	0.79	2.19	1.50	1.00	0.09	3.28	0.39	99.54
KM-34	80.95	0.25	8.18	1.01	0.69	0.03	1.69	1.60	1.28	1.22	0.09	2.32	0.28	99.59
KM-37	68.55	0.42	12.18	0.06	3.10	0.06	2.91	2.79	1.62	2.55	0.23	4.98	0.10	99.55
KM-46	73.35	0.20	8.17	0.30	2.85	0.07	1.49	4.57	1.22	1.29	0.05	5.51	0.39	99.46
KM-57	66.00	0.66	16.19	0.29	2.48	0.02	2.64	1.85	1.93	3.49	0.13	3.84	0.17	99.69
KM-329	69.43	0.47	11.09	1.77	1.73	0.05	1.29	3.60	2.02	1.84	0.15	5.62	0.58	99.64
KM-333	78.50	0.29	8.81	0.58	1.97	0.01	1.71	1.68	1.29	1.98	0.10	3.10	0.05	100.07
KM-64	75.02	0.32	9.68	0.93	2.29	0.10	1.27	2.43	0.48	3.44	0.12	3.60	0.20	99.88
KM-67	74.57	0.32	8.15	1.05	1.39	0.20	3.12	3.57	1.39	1.62	0.05	4.07	0.28	99.78
KM-69	77.75	0.33	11.14	0.93	0.40	0.03	1.00	1.22	1.46	2.61	0.16	2.52	0.37	99.92
KM-76	71.80	0.39	11.26	1.04	2.62	0.12	1.24	2.04	1.26	2.67	0.09	4.72	0.31	99.56
KM-79	72.32	0.38	11.46	1.81	3.08	0.04	2.40	0.56	2.47	2.16	0.13	2.35	0.45	99.61
KM-213	72.82	0.58	14.21	1.28	1.21	0.02	1.00	0.28	1.68	2.90	0.24	3.05	0.16	99.43
KM-223	80.19	0.22	8.52	1.97	1.79	0.03	1.40	0.14	1.99	1.23	0.10	1.75	0.25	99.58
KM-321	74.92	0.43	11.14	0.40	2.43	0.04	1.31	2.24	2.06	2.12	0.08	2.48	0.32	99.97
KM-322	74.11	0.41	11.18	0.80	2.34	0.04	2.80	0.69	1.83	2.54	0.12	2.81	0.09	99.76
KM-725	79.35	0.30	9.15	0.30	2.25	0.06	1.08	0.65	2.39	1.68	0.11	2.05	0.24	99.61
KM-730	74.90	0.29	10.28	2.39	1.23	0.04	1.18	1.23	2.64	2.54	0.16	2.66	0.31	99.85
KM-739	82.80	0.17	7.56	0.42	1.85	0.03	0.83	0.56	2.91	1.85	0.07	0.27	0.28	99.60

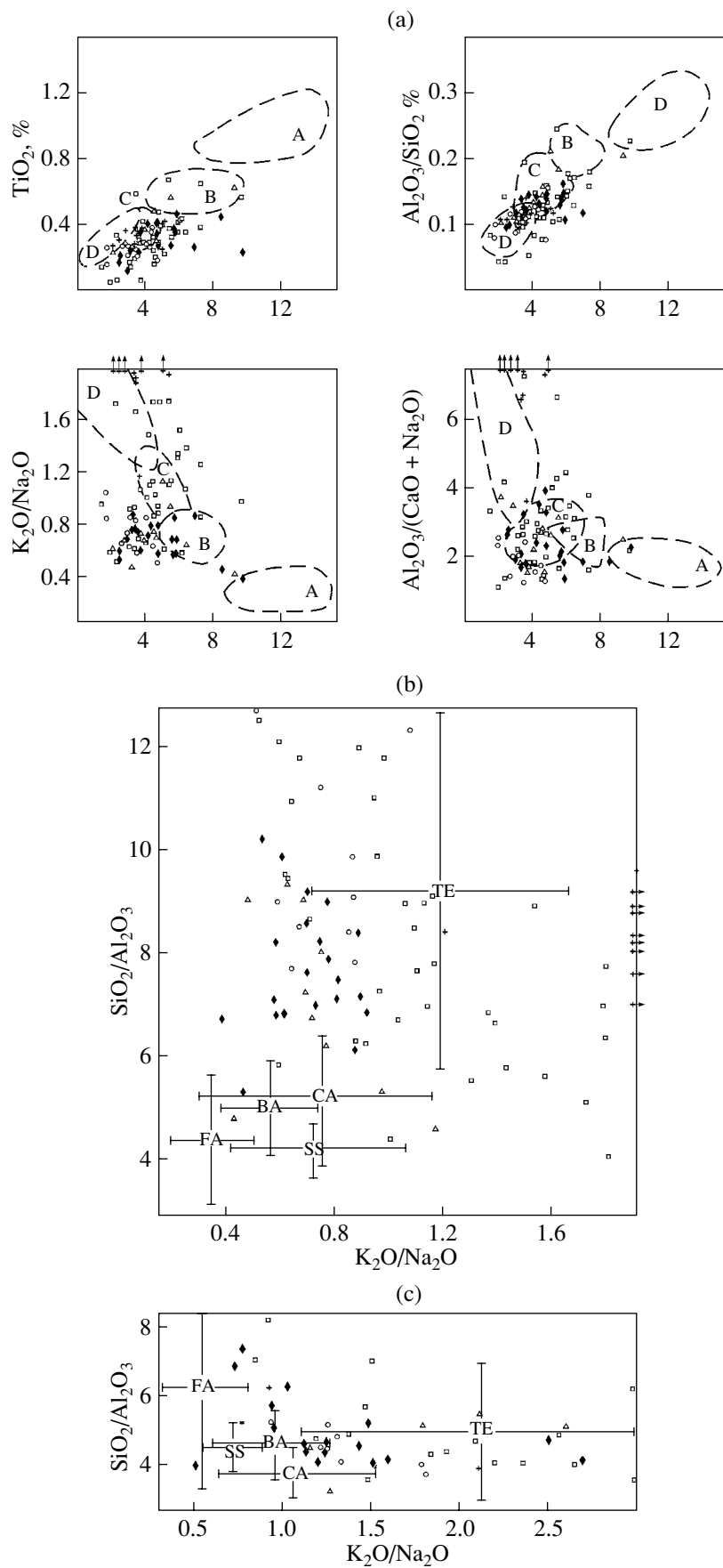
**Table 2.** (Contd.)

Sample no.	SiO <sub>2</sub>	TiO <sub>2</sub>	Al <sub>2</sub> O <sub>3</sub>	Fe <sub>2</sub> O <sub>3</sub>	FeO	MnO	MgO	CaO	Na <sub>2</sub> O	K <sub>2</sub> O	P <sub>2</sub> O <sub>5</sub>	L.O.I.	H <sub>2</sub> O <sup>-</sup>	Total
KM-741	62.20	0.56	14.11	1.88	4.72	0.09	3.09	3.56	2.96	2.97	0.17	2.40	0.84	99.55
KM-742	63.70	0.64	11.49	1.17	4.10	0.08	2.03	4.76	2.36	3.07	0.16	6.01	0.33	99.90
KM-743	75.70	0.24	9.68	1.86	1.48	0.05	1.15	1.03	2.55	2.97	0.12	2.48	0.30	99.61
KM-744	69.60	0.35	12.01	2.58	2.05	0.07	1.80	1.77	2.10	3.00	0.14	3.86	0.36	99.66
KM-801	72.72	0.35	10.61	2.24	1.93	0.08	1.76	0.96	2.41	3.29	0.12	2.48	0.55	99.50
KM-804	80.40	0.19	8.47	1.56	0.97	0.06	0.87	0.13	3.07	1.89	0.06	1.40	0.44	99.52
KM-809	74.59	0.35	9.73	2.26	2.12	0.06	2.02	1.43	2.39	2.63	0.12	2.23	0.26	100.19
KM-816	85.60	0.14	7.27	0.68	0.30	0.02	0.50	0.41	1.78	1.74	0.09	1.23	0.17	99.93
KM-900B	88.71	0.06	3.94	1.92	0.11	0.03	0.33	1.32	1.57	0.81	0.05	0.93	0.15	99.99
KM-900B	88.71	0.06	3.94	1.92	0.11	0.03	0.33	1.32	1.57	0.81	0.05	0.93	0.15	99.99
KM-901	86.99	0.05	3.93	1.49	0.08	0.04	0.40	1.98	1.58	0.93	0.06	2.28	0.90	99.90
KM-902	85.11	0.06	4.60	3.50	0.15	0.09	0.11	1.35	1.21	1.32	0.10	2.64	0.15	100.39
<i>Middle Subformation</i>														
KM-97	80.59	0.29	8.85	1.18	0.57	0.03	1.10	0.63	1.89	1.29	1.10	2.16	0.09	99.77
KM-108	65.09	0.40	13.92	2.55	1.30	0.08	1.20	2.98	2.26	2.64	0.15	6.48	0.57	99.62
KM-109	74.39	0.37	10.19	2.69	0.67	0.12	0.67	2.59	1.98	1.36	0.23	4.38	0.37	100.01
KM-571	82.24	0.23	8.74	0.99	0.44	0.02	0.70	0.42	1.90	1.18	0.07	2.52	0.18	99.63
KM-570	66.14	0.62	13.60	1.90	3.62	0.06	3.79	1.88	3.52	1.49	0.14	2.05	0.65	99.46
KM-705	69.72	0.30	10.23	1.76	1.60	0.12	1.32	4.61	2.23	1.59	0.63	5.64	0.37	100.12
KM-716	68.62	0.56	12.73	3.14	1.19	0.10	1.17	1.77	2.25	2.18	0.30	5.39	0.07	100.11
KM-717	78.66	0.27	8.63	1.77	0.70	0.04	0.79	2.48	2.25	1.07	0.09	3.51	0.42	100.08
KM-718	72.16	0.48	11.48	1.02	2.20	0.07	1.35	1.75	2.31	1.76	0.17	4.62	0.56	99.93
KM-719	75.00	0.29	9.27	1.34	1.17	0.07	1.21	3.30	1.88	1.40	0.20	4.70	0.42	100.25
<i>Upper Subformation</i>														
KM-132	72.66	0.38	9.43	1.21	1.95	0.06	1.30	3.34	2.09	1.33	0.16	5.12	0.38	99.41
KM-135	72.59	0.29	9.28	1.19	1.09	0.08	1.86	3.90	2.12	1.85	0.09	4.74	0.49	99.57
KM-143	85.01	0.16	6.92	1.03	0.20	0.05	0.51	1.07	1.65	1.77	0.03	1.52	0.19	100.11
KM-153	80.75	0.21	7.19	1.09	0.63	0.02	1.25	1.17	2.59	1.93	0.03	2.23	0.62	99.71
KM-176	79.09	0.21	8.78	1.60	1.16	0.03	0.80	0.83	2.81	1.64	0.08	1.83	0.57	99.43
KM-187	77.45	0.18	6.10	1.05	1.43	0.04	2.25	3.10	1.70	0.86	0.03	5.26	0.41	99.86
KM-304	81.33	0.26	8.23	1.39	0.19	0.03	0.20	1.95	1.60	1.38	0.07	2.54	0.36	99.53
KM-306	77.51	0.27	8.52	0.93	1.16	0.09	1.09	2.29	1.87	1.62	0.10	4.30	0.30	100.05
KM-314	71.97	0.25	8.55	1.22	1.24	0.08	1.01	5.19	1.71	1.45	0.10	6.54	0.36	99.67
KM-316	74.65	0.27	8.77	1.36	0.70	0.07	0.60	4.19	2.05	1.36	0.09	5.30	0.30	99.71
<i>Luzhki Formation</i>														
KM-846	82.58	0.27	8.82	1.04	0.52	0.03	0.56	0.23	0.15	2.61	0.12	2.38	0.49	99.80
KM-847	81.48	0.38	8.49	0.94	1.15	0.05	1.49	0.14	1.26	2.49	0.05	1.88	0.40	100.00
KM-849	81.73	0.30	8.84	0.56	1.22	0.03	0.72	0.22	0.16	3.57	0.08	1.93	0.23	99.59
KM-851	79.57	0.36	10.16	1.52	0.50	0.03	0.81	0.18	0.19	3.55	0.10	2.28	0.33	99.58
KM-852	78.15	0.41	9.33	2.72	0.68	0.07	1.77	0.19	1.00	2.62	0.10	2.45	0.32	99.81
KM-854	76.61	0.25	9.63	0.81	1.41	0.11	2.81	0.68	0.27	3.75	0.05	2.69	0.42	99.49
KM-855	77.40	0.36	11.03	1.30	1.52	0.04	0.82	0.39	1.28	2.97	0.10	2.15	0.21	99.57
KM-856	81.50	0.28	8.55	1.59	0.75	0.04	0.99	0.30	0.15	3.44	0.10	1.77	0.41	99.87
KM-859	79.23	0.36	9.45	1.52	1.12	0.02	1.17	0.52	2.08	2.58	0.09	1.59	0.20	99.93
<i>Clayey rocks</i>														
<i>Meandrovyi Formation</i>														
KM-907	68.42	0.48	14.68	1.64	2.51	0.06	0.72	1.52	2.33	2.94	0.24	3.73	0.24	99.51
KM-917	65.71	0.47	15.79	1.98	2.82	0.06	1.14	2.10	1.04	2.80	0.27	5.42	0.41	100.01
KM-918	71.29	0.30	9.68	1.53	4.01	0.12	1.54	2.84	1.76	1.37	0.11	4.72	0.23	99.50
KM-920	68.74	0.48	13.19	0.87	3.98	0.04	0.48	1.99	2.01	2.99	0.12	4.33	0.28	99.50

**Table 2.** (Contd.)

Sample no.	SiO <sub>2</sub>	TiO <sub>2</sub>	Al <sub>2</sub> O <sub>3</sub>	Fe <sub>2</sub> O <sub>3</sub>	FeO	MnO	MgO	CaO	Na <sub>2</sub> O	K <sub>2</sub> O	P <sub>2</sub> O <sub>5</sub>	L.O.I.	H <sub>2</sub> O <sup>-</sup>	Total
KM-929	66.91	0.48	14.13	1.53	3.09	0.07	1.59	1.76	0.78	2.76	0.20	6.51	0.39	100.15
KM-937	64.41	0.69	15.76	3.94	1.97	0.04	1.18	0.80	1.84	2.78	0.37	4.99	0.83	99.63
KM-944	63.78	0.66	15.64	4.54	1.53	0.04	1.09	1.23	2.30	2.77	0.30	4.98	0.70	99.54
KM-947	67.30	0.62	14.58	2.25	2.78	0.04	0.76	0.94	2.22	2.50	0.24	4.84	0.68	99.75
KM-949	64.36	0.60	14.13	1.36	3.51	0.04	1.30	1.77	1.80	2.58	0.28	7.12	0.77	99.62
KM-758	65.40	0.70	15.66	2.90	1.64	0.04	1.61	0.65	2.27	3.64	0.16	4.48	0.62	99.77
KM-759	61.02	0.63	15.31	2.17	5.10	0.08	3.10	1.99	3.54	1.82	0.20	3.94	0.54	99.44
KM-763	71.42	0.33	10.41	4.19	0.80	0.06	1.48	2.16	2.32	1.71	0.16	4.52	0.34	99.90
KM-769	66.64	0.73	15.11	2.06	2.91	0.04	1.30	0.79	2.21	2.51	0.26	4.74	0.53	99.83
KM-774	65.60	0.73	15.01	2.07	2.72	0.04	1.49	1.18	2.15	2.69	0.22	5.22	0.63	99.75
KM-778	71.00	0.47	12.42	1.41	2.74	0.05	1.31	1.50	2.29	2.16	0.18	4.40	0.40	100.33
KM-779	70.90	0.35	11.27	1.27	3.33	0.13	2.21	1.61	1.90	1.96	0.14	4.04	0.37	99.48
KM-784	67.46	0.49	13.28	1.83	2.48	0.04	1.35	2.42	2.39	2.29	0.24	5.14	0.55	99.96
Kema Formation														
Lower Subformation														
KM-1	64.11	0.54	13.64	1.57	3.27	0.06	4.34	1.30	1.66	3.47	0.19	5.23	0.12	99.50
KM-2	76.02	0.27	9.25	1.55	2.53	0.06	1.70	1.67	1.29	1.19	0.07	3.29	0.51	99.40
KM-9	64.69	0.69	14.95	1.54	3.74	0.05	1.80	1.63	1.55	2.85	0.19	4.85	0.85	99.38
KM-11	74.22	0.40	10.54	1.26	2.93	0.08	1.32	1.85	1.69	1.44	0.15	3.51	0.44	99.83
KM-12	64.20	0.71	15.91	1.91	3.56	0.03	2.02	0.56	1.22	3.23	0.15	5.07	0.73	99.30
KM-50	71.50	0.39	10.17	1.27	2.77	0.07	1.70	3.20	1.56	2.35	0.14	3.89	0.41	99.42
KM-71	72.98	0.48	11.86	0.81	2.61	0.04	1.30	0.42	1.03	3.13	0.11	4.21	0.59	99.57
KM-77	69.60	0.61	14.21	1.97	2.22	0.03	1.49	0.27	1.34	3.43	0.12	3.45	0.75	99.49
KM-210	69.29	0.54	14.00	0.70	3.68	0.07	1.47	1.69	2.22	3.05	0.11	2.81	0.12	99.75
KM-724	62.03	0.80	17.32	1.82	3.74	0.09	2.29	0.60	2.19	3.25	0.29	4.72	0.54	99.68
KM-726	63.68	0.84	17.72	2.20	2.19	0.03	1.30	0.15	1.35	4.05	0.29	5.00	0.83	99.62
KM-747	63.80	0.70	15.66	2.14	2.56	0.07	1.63	1.57	0.67	4.86	0.19	5.16	0.58	99.60
KM-750	63.90	0.70	14.52	0.82	3.90	0.04	1.74	2.00	2.00	3.85	0.17	5.27	0.78	99.69
KM-755	68.80	0.58	12.10	0.65	3.28	0.05	1.55	2.00	2.09	3.07	0.17	4.86	0.59	99.79
KM-805	67.53	0.57	14.25	4.32	1.10	0.04	1.13	0.86	2.37	2.82	0.21	3.93	0.62	99.75
KM-807	64.70	0.63	15.97	3.18	2.15	0.03	1.73	1.12	1.50	3.54	0.15	4.14	0.71	99.55
Middle Subformation														
KM-121	56.54	0.60	17.26	2.26	3.67	0.06	3.83	3.58	2.63	3.35	0.17	4.92	0.71	99.58
KM-128	66.55	0.64	12.94	4.65	1.81	0.13	0.91	1.02	1.41	2.53	0.10	6.46	0.36	99.51
KM-706	67.51	0.58	14.96	3.56	0.90	0.06	1.32	0.25	2.02	2.31	0.26	4.96	1.13	99.82
KM-707	67.50	0.45	12.19	3.63	0.50	0.06	0.90	3.76	0.90	1.90	0.15	6.97	0.74	99.67
KM-712	67.41	0.60	13.22	3.19	0.89	0.12	1.24	2.18	0.77	2.20	0.37	6.80	0.97	99.96
Upper Subformation														
KM-131	65.59	0.52	12.51	2.76	1.78	0.05	3.40	1.65	2.67	2.52	0.14	6.14	0.38	100.11
KM-133	66.74	0.59	13.88	1.42	3.24	0.03	1.41	1.68	2.05	2.69	0.13	4.80	0.80	99.46
KM-139	67.20	0.51	15.06	0.27	3.39	0.14	0.34	2.49	1.93	2.43	0.11	5.34	0.38	99.59
KM-146	67.99	0.58	13.17	1.80	2.24	0.03	2.20	0.84	2.10	2.65	0.12	4.82	0.88	99.42
KM-149	65.89	0.63	14.56	1.31	2.09	0.04	2.53	1.53	1.87	2.28	0.10	6.24	0.49	99.56
KM-189	62.47	0.72	15.39	3.39	1.67	0.04	2.26	1.42	2.20	2.95	0.22	6.69	0.35	99.77
KM-194	61.76	0.69	15.41	1.52	3.10	0.04	2.01	1.51	1.73	3.09	0.20	7.72	0.84	99.62
KM-196	60.34	0.70	16.14	1.34	3.52	0.04	2.03	1.53	1.95	3.53	0.12	7.31	1.07	99.62
Luzhki Formation														
KM-857	72.52	0.37	11.62	1.51	1.35	0.05	1.20	3.93	2.37	2.20	0.12	2.10	0.19	99.53
KM-858	64.13	0.68	16.39	3.59	1.35	0.03	1.52	0.82	1.74	3.67	0.26	5.35	0.61	100.14

Note: Analyses were performed at the Far East Geological Institute (V.N. Kaminskaya, L.A. Vrzhosek, and G.I. Makarova, analysts).



turn, is governed by tectonic settings of their formation. Principles of the genetic interpretation of chemical composition are similar to those for the rock-forming components (Fig. 9). In Fig. 9a based on (Bhatia, 1983), sandstones are classified according to tectonic settings. One can see that most Kema sandstones either correspond to or approximate sandstones from active continental margins and basins conjugated with island arcs built on continental crust. The data points not exactly fall into the continental island-arc field due to the low ( $\text{Fe} + \text{Mg}$ ) contents. This is caused by the high maturity of rocks owing to the enrichment in quartz and siliceous rocks. In Fig. 9b, based on (Maynard *et al.*, 1982), data points of sandstones are scattered, but they are nearer to sands from passive continental margins or continental-margin arcs. The deviation of data points from fields of active continental margin and continental-margin arcs is explained by the atypical predominance of K over Na in the studied sandstones owing to the abundance of high-K basalt (shoshonite) fragments.

#### *Clayey Rocks*

Depending on the lithological composition (siltstones, mudstones, and silty mudstones), the content of silty clasts varies from 5 to 70–80 vol %. Rocks are typically well sorted, although some varieties are less sorted because of uneven (patchy) distribution of silty clasts. Rounded and subrounded silty grains are represented by quartz, feldspars, and less common cherts, volcanic rocks, fine-clastic rocks, biotite, volcanic glass, and ore minerals. Fine detritus and carbonaceous lenses are rather abundant.

Clay rocks are chemically similar to sandstones but differ in lower  $\text{SiO}_2$  (from 56.54 to 72.23%) and  $\text{CaO}$  (0.15–3.76%) and higher  $\text{TiO}_2$  (0.27–0.84%),  $\text{Al}_2\text{O}_3$  (9.25–17.72%),  $\text{FeO} + \text{Fe}_2\text{O}_3$  (3.4–7.27%),  $\text{MgO}$  (0.48–4.43%),  $\text{Na}_2\text{O}$  (0.78–3.56%), and  $\text{K}_2\text{O}$  (1.19–4.86%). Paleotectonic interpretation of chemical composition as presented in the diagram of Maynard (Maynard *et al.*, 1982) (Fig. 9b) is similar to but more certain than that based on sandstone composition. Most data points of clay rocks are clustered in the fields of active continental margins and continental island arcs.

#### *Coarse-Clastic Rocks*

Coarse-clastic rocks (conglomerates and gritstones) bear abundant information on the composition and tectonic nature of provenances. Therefore, one can sometimes reliably identify all provenances and even their age. They occur at different levels of the studied section

and are most abundant (50–60 vol %) in the Lower Kema Subformation.

Conglomerates are fine- to medium-pebble (1–5 cm), occasionally coarse-pebble (up to 10–15 cm) rocks with some boulders reaching 20–40 cm. The typically equant or elongated clastic component (70–85 vol %) is medium- to well-sorted and rounded. Gritstones are mainly medium- to coarse-gravel (clasts from 3 to 10 mm in size), more rarely fine-gravel (to 3 mm) rocks. Occasionally, they contain well-rounded pebbles and boulders of volcanic rocks (up to 10–40 cm), as well as disoriented siltstone clasts (up to 30 cm). The clastic component accounts for 60–80 vol %. Gritstones are typically medium- to well-sorted, while gravel grains are rounded or subrounded.

Conglomerates and gritstones mainly contain large pebbles of volcanic rocks (30–60%) and fine pebbles of cherts (30–70%). Clasts of sedimentary rocks (10–30%) and metamorphosed cherts are less common. Large grains and fragments of quartz and plagioclase are rare in the matrix. Petrographically, volcanic pebbles are identical to island-arc basalts of the Kema Formation. Siliceous pebbles occasionally contain a significant amount of radiolarian skeletons. Radiolarians were separated from pebbles in order to determine the age of provenances for the Kema sedimentary paleobasin. I.V. Kemkin determined the following radiolarians: *Archaeospongoprunum* sp., *Archaeodictyomitra minoenensis* (Mizutani), *Archycapsa pachyderma* Tan Sin Hok, *Pseudodictyomitra carpatica* (Lozyniak), *Pseudodictyomitra primitive* Matsuoka et Yao, *Parvingula boesii* gr. (Parona), *Plafkerium* sp., *Stylosphaera* sp., *Sethocapsa funatoensis* Aita, *Sethocapsa* sp., *Capnodoce* sp., *Capnuchosphaera* sp., *Obesacapsula cetia* (Foreman), *Tricolocapsa* sp., and *Tritrabs* sp. These fauna define the age of parental rocks as Triassic–Late Jurassic.

Thus, gritstones and conglomerates mainly include clasts of island-arc volcanic rocks and cherts with Triassic and Jurassic radiolarians. This suggests the possible erosion of two main sources of clastic material: volcanic island arc and its basement represented by the Jurassic–Early Cretaceous accretionary prism similar to prisms of the Samarka and Taukhin terranes of Sikhote Alin (Khanchuk *et al.*, 1995; Malinovsky *et al.*, 2002).

Thus, the composition of terrigenous rocks and its genetic interpretation show that Early Cretaceous sediments accumulated at the active continental margin, more probably, in a basin conjugated to the continental (ensialic) island arc.

**Fig. 9.** Chemical compositions of sandy and clayey rocks from different geodynamic settings. (a) Basin types (Bhatia, 1983). Dashed lines are fields of ancient sandstones in basins related to (A) oceanic island arcs, (B) continental island arcs, (C) active continental margin, (D) passive continental margins. ( $\text{Fe}_2\text{O}_3^*$ ) Total iron. (B, C) Basin settings for sandstones and clayey rocks, respectively (Maynard *et al.*, 1982). Intersecting lines are standard deviations from average compositions of recent deep-water sands and clays in different geodynamic settings. Symbols and abbreviations are as in Fig. 3.

## SETTINGS AND ACCUMULATION CONDITIONS OF TERRIGENOUS ROCKS

Lower Cretaceous rocks of the Kema River basin mainly consist of rhythmically intercalated sandstones and siltstone. The rhythms show graded bedding, sharp erosional bases, and Bouma successions *abced*, *abde*, *ade*, *bde*, *bcde*, and *cde*. All these features are typical of turbidites. The turbidites are usually associated with slump deposits, mixtites, sandstones, gritstones, and fine-gravel conglomerates connected by gradual transitions. Normal and inverse grading of coarse-clastic rocks with siltstone clasts and plant detritus, which occasionally occurs as interbeds up to 30 cm thick, indicate the deposition by high-density (granular) and debris flows. The debris flows evidently formed mixtite horizons that are characterized by chaotic structure, high matrix content, and absence of sorting. In addition, the section also includes siltstone layers with sandstone interlayers formed by bottom currents. Such a genetic set of sediments suggests their accumulation in the lower part and near the base of submarine slope and in the adjacent areas of basin plain. The clastic material was mainly transported and deposited in the Kema sedimentary basin by gravitational flows varying in density, composition, and origin. The direction of these flows can be deduced from slump deformations found in turbidites at different levels of the section. Their analysis indicates a northeastern strike of the submarine slope that accumulated the sediments, while clastic material was transported from southeast to northwest (Malinovsky *et al.*, 2002).

Genetic interpretation of the composition of terrigenous rocks indicates that clastic material was mainly derived from the volcanic island arc with basement composed of continental crust fragment containing Jurassic–Early Cretaceous accretion prism. The fragment, probably advanced toward ocean along a major fault, was large enough to supply a large amount of clastic material and its surface was located, at least partially, above the sea level. This is indicated by a significant amount of land plant remains in the terrigenous rocks. The Kema basalts, associated with terrigenous and pyroclastic rocks, chemically belong to the island-arc type of high-K calc-alkaline and shoshonite series, which formed in the rear zone of the island arc at the final stages of its formation (Malinovsky *et al.*, 2003).

## CONCLUSIONS

Thus, the composition, structure, and some textural features of terrigenous rocks and associated volcanic rocks suggest that the mature Moneron–Samarga volcanic island arc existed along the eastern margin of Asia in the Barremian (?)–Albian. Thick gravitational sequences accumulated in the rear zone of the arc. In the Aptian–early Albian, their accumulation was accompanied by active back-arc basaltic volcanism. The island-arc front is located in the eastern side within

the Rebun–Kabato terrane (Hokkaido, Rebun, and Moneron Islands) with a thick sequence of calc-alkaline lavas and pyroclastics (Simanenko, 1991).

Northwest of the Kema terrane, accumulation of Early Cretaceous terrigenous rocks (turbidites of the Zhuravlev terrane) coincided with large-scale movements along sinistral strike slips that separate the continental and oceanic plates. The association of terranes with different types of interaction between continental and oceanic plates (subduction and transform sliding) within a single continental margin is the characteristic feature of at least the Early Cretaceous stage of evolution of the eastern margin of Asia.

## ACKNOWLEDGMENTS

We are grateful to P.V. Markevich for consultation and constructive comments during the manuscript preparation.

This study was supported by the Russian Foundation for Basic Research (project nos. 01-05-64602 and 02-05-65326).

## REFERENCES

- Arai, S., Chemistry of Chromian Spinel in Volcanic Rocks as a Potential Guide to Magma Chemistry, *Miner. Mag.*, 1992, vol. 56, pp. 173–184.
- Bhatia, M.R., Plate Tectonics and Geochemical Composition of Sandstones, *J. Geol.*, 1983, vol. 91, no. 6, pp. 611–627.
- Dickinson, W.R. and Suczek, C.A., Plate Tectonics and Sandstone Composition, *Am. Assoc. Petrol. Geol.*, 1979, vol. 63, no. 12, pp. 2164–2182.
- Khanchuk, A.I., Ratkin, V.V., Ryazantseva, M.D., Golozubov, V.V., and Gonokhova, N.G., *Geologiya i poleznye iskopayemye Primorskogo kraya: ocherk* (Geology and Mineral Resources of the Primorye Region), Vladivostok: Dal'nauka, 1995.
- Kovalenko, S.V., Lower Cretaceous Volcanosedimentary Rock Associations in the Middle Sikhote Alin Region, in *Vulkanogennoe i vulkanogenno-osadochnye porody Dal'nego Vostoka* (Volcanic and Volcanosedimentary Rocks in the Russian Far East), Vladivostok: Dal'nevost. Nauchn. Tsentr Akad. Nauk SSSR, 1985, pp. 100–115.
- Kumon, F. and Kiminami, K., Modal and Chemical Compositions of the Representative Sandstones from Japanese Islands and Their Tectonic Implications, *Proceedings of 29th Int. Geol. Congr.*, 1994, part A, pp. 131–137.
- Leterrier, J., Maury, R.C., and Thonon, P., Clinopyroxene Composition as a Method of Identification of the Magmatic Affinities of Paleo-Volcanic Series, *Earth Planet. Sci. Lett.*, 1982, vol. 59, pp. 139–154.
- Malinovsky, A.I., Filippov, A.N., Golozubov, V.V., Simanenko, V.P., and Markevich V.S., Lower Cretaceous Rocks in the Kema River Basin (Eastern Sikhote Alin): Sedimentary Cover of the Back-Arc Basin, *Tikhookean. Geol.*, 2002, vol. 21, no. 1, pp. 52–66.
- Malinovsky, A.I., Golozubov, V.V., and Simanenko, V.P., The Kema Terrane (Eastern Sikhote Alin): A Back-Arc Basin Fragment, in *Geodinamika, magmatizm i minerageniya kon-*

- tinental'nykh okrain Severa Patsifiki* (Geodynamics, Magmatism, and Mineralization of Continental Margins in the North Pacific), Magadan: Severovost. Kompl. Nauchno-Issled. Inst. Dal'nevost. Otd. Ross. Akad. Nauk, 2003, vol. 1, pp. 196–199.
- Markevich, P.V., Filippov, A.N., Malinovsky, A.I., et al., *Melovye vulkanogenno-osadochnye obrazovaniya Nizhnego Priamur'ya* (Cretaceous Volcanosedimentary Rocks of the Lower Amur Region), Vladivostok: Dal'nauka, 1997.
- Markevich, P.V., Malinovsky, A.I., Golozubov, V.V., et al., Early Cretaceous Paleogeography of the Southern Russian Far East, in *Geodinamika i metallogeniya* (Geodynamics and Metallogeny), Vladivostok: Dal'nauka, 1999, pp. 49–63.
- Markevich, P.V., Konovalov, V.P., Malinovsky, A.I., and Filippov, A.N., *Nizhnemelovye otlozheniya Sikhote-Alinya* (Lower Cretaceous Rocks of the Sikhote Alin Region), Vladivostok: Dal'nauka, 2000.
- Maynard, J.B., Valloni, R., and Yu, H.S., Composition of Modern Deep-Sea Sands from Arc-Related Basins, in *Trench-Forearc Geology. Sedimentation and Tectonics of Modern and Ancient Plate Margins*, Oxford: Blackwell Sci. Publ., 1982, pp. 551–561.
- Nechaev, V.P., Evolution of the Philippine and Japan Seas from the Clastic Sediment Record, *Mar. Geol.*, 1990, no. 97, pp. 167–190.
- Nechaev, V.P. and Ispphording, W.C. Heavy-Mineral Assemblages of Continental Margins as Indicators of Plate-Tectonic Environments, *J. Sed. Petrol.*, 1993, vol. 63, no. 6, pp. 1110–1117.
- Nechaev, V.P., Markevich, P.V., Malinovsky, A.I., Philippov, A.N., and Vysotsky, S.V., Tectonic Settings of Deposition of the Cretaceous Sediments from the Lower Amur Region, Russian Far East, *J. Sed. Soc. Japan*, 1996, no. 43, pp. 69–81.
- Nisbet, E.G. and Pearce, J.A., Clinopyroxene Composition in Mafic Lavas from Different Tectonic Settings, *Contrib. Mineral. Petrol.*, 1977, no. 63, pp. 149–160.
- Ruzhentsev, S.V. and Khvorova, I.V., The Middle Paleozoic Olistostrome in the Sakmara Zone, Southern Urals, *Litol. Polezn. Iskop.*, 1973, vol. 8, no. 6, pp. 21–32.
- Shutov, V.D., Classification of Sandstones, *Litol. Polezn. Iskop.*, 1967, no. 5, pp. 86–102.
- Simanenko, V.P., Late Mesozoic Volcanic Arcs in Eastern Sikhote Alin and Sakhalin, *Tikhookean. Geol.*, 1986, no. 1, pp. 7–13.
- Simanenko, V.P., Basalt–Andesite Rock Association of Paleozoic and Mesozoic Island Arcs, in *Tikhookeanskaya okraina Azii. Magmatizm* (Pacific Margin of Asia: Magmatism), Moscow: Nedra, 1991, pp. 58–72.
- Sokolov, S.D., *Olistostromovye tolshchi i ofiolitovye pokrovy Malogo Kavkaza* (Olistostrome Sequences and Ophiolitic Nappes in the Lesser Caucasus), Moscow: Nauka, 1977.